CONVERSION OF *n*-PENTANE TO AROMATICS: EFFECT OF SURFACE MODIFICATION BY CHEMICAL LIQUID DEPOSITION AND PROMOTER OVER NANO SCALE Ga/HZSM-5

Sukkatad Sintapanin

A Thesis Submitted in Partial Fulfilment of the Requirements
for the Degree of Master of Science
The Petroleum and Petrochemical College, Chulalongkorn University
in Academic Partnership with
The University of Michigan, The University of Oklahoma,
Case Western Reserve University, and Institut Français du Pétrole
2018

บทคัดย่อและแฟ้มข้อมูลฉบับเต็มของวิทยานิพนธ์ตั้งแต่ปีการศึกษา 2554 ที่ให้บริการในคลังปัญญาจุฬาฯ (CUIR)
เป็นแฟ้มข้อมูลของนิสิตเจ้าของวิทยานิพนธ์ที่ส่งผ่านทางบัณฑิตวิทยาลัย
The abstract and full text of theses from the academic year 2011 in Chulalongkorn University Intellectual Repository(CUIR)
are the thesis authors' files submitted through the Graduate School.

Thesis Title: Conversion of *n*-Pentane to Aromatics: Effect of Surface

Modification by Chemical Liquid Deposition and Promoter

over Nano Scale Ga/HZSM-5

By: Sukkatad Sintapanin

Program: Petroleum Technology

Thesis Advisor: Assoc. Prof. Siriporn Jongpatiwut

_____

Accepted by The Petroleum and Petrochemical College, Chulalongkorn University, in partial fulfilment of the requirements for the Degree of Master of Science.

.... College Dean

(Prof. Suwabun Chirachanchai)

Thesis Committee:

....

(Assoc. Prof. Siriporn Jongpatiwut)

....

(Prof. Pramoch Rangsunvigit)

....

(Dr. Sitthiphong Pengpanich)

ABSTRACT

This work studied the effects of chemical liquid deposition, i.e., TEOS concentration and multicycle silylation on Ga/HZSM-5 on their catalytic performance in aromatization of *n*-pentane. The parent nano scale HZSM-5 zeolite catalysts were incorporated with Ga by impregnation method followed by silylation via chemical liquid deposition (CLD) using tetraethyl orthosilicate (TEOS) by varying concentrations and number of cycles. Moreover, the small amount of Pt, Zn, La and P was introduced by co-impregnation method to study the effect of promoter. The physical and chemical properties of catalysts were characterized by N_2 physisorption, XRD, NH_3-TPD, IPA-TPD, TPO, TPR, SEM and ^{27}Al MAS NMR techniques. Catalytic activity was tested in a continuous flow fixed-bed reactor at 500 °C, atmospheric pressure, and WHSV of 5 h^{-1}. The results indicated that the addition of Ga greatly improved the aromatics selectivity due to the presence of GaO^+ species which acted as active site for dehydrogenation reaction. The TEOS concentration slightly increased the *p*-xylene selectivity while multicycle silylation significantly improved the *p*-xylene in mixed xylenes due to the formation of uniformity inert silica layer. The silylated catalyst exhibited the lower of *n*-pentane conversion resulting from its lower external acid sites. The co-impregnation with P promoted the aromatics selectivity because there was formation of SAPO interfaces, pentahedrally aluminium framework and medium acid sites.

บทคัดย่อ

ศุขธัช สินธพานินท์ : การเปลี่ยนสภาพสารนอร์มัลเพนเทนให้เป็นสารอะโรเมติกส์โดย
ผลกระทบของการปรับปรุงพื้นที่ผิวโดยการตกเคลือบด้วยสารละลายเคมีและการเติมตัวสนับสนุนบน
ต่อตัวเร่งปฏิกิริยาโลหะแกลเลียมบนตัวรองรับซีโอไลต์ชนิดแซดเอสเอ็ม-5 ขนาดนาโน
(Conversion of *n*-Pentane to Aromatics: Effect of Surface Modification by Chemical
Liquid Deposition and Promoter over Nano Scale Ga/HZSM-5)
อ. ที่ปรึกษา : รศ. ดร. ศิริพร จงผาติวุฒิ 73 หน้า

การเปลี่ยนสารนอร์มัลเพนเทนให้เป็นสารอะโรเมติกส์ได้ถูกศึกษาบนตัวเร่งปฏิกิริยาซี
โอไลท์ชนิด แซดเอสเอ็ม-5 (ZSM-5) ขนาดนาโน ตัวเร่งปฏิกิริยาถูกเติมแบบเปียกพอดีกับโลหะ
แกลเลียมและกระบวนการไซริเลชันผ่านการเคลือบด้วยเทคนิคสารละลายเคมี (CLD) ที่เตรียมจากเต
ตระ-เอทิลออโธซิลิเกต (TEOS) 2 ปัจจัย ได้แก่ เตตระเอทิลออโธซิลิเกต และจำนวนรอบของการ
เคลือบ นอกจากนี้ยังศึกษาผลกระทบของตัวสนับสนุน ได้แก่ แพลตตินัม สังกะสี แลนทานัม และ
ฟอสฟอรัสต่อโลหะแกลเลียมบนตัวรองรับ ZSM-5 ด้วยวิธีเติมแบบเปียกร่วม โดยได้มีการศึกษา
คุณสมบัติทางเคมีและทางกายภาพของตัวเร่งปฏิกิริยาด้วยวิธีต่าง ๆ ได้แก่ BET XRD NH$_3$-TPD
IPA-TPD TPO TPR SEM และ ^{27}Al MAS NMR โดยการศึกษาประสิทธิภาพของตัวเร่งปฏิกิริยาทำ
ในเครื่องปฏิกรณ์เบดนิ่งแบบไหลต่อเนื่องที่อุณหภูมิ 500 องศาเซลเซียสภายใต้ความดันบรรยากาศ
ด้วยอัตราส่วนของสารป้อนต่อตัวเร่งปฏิกิริยาโดยน้ำหนัก (WHSV) เท่ากับ 5 ต่อชั่วโมง จากผลการ
ทดลองพบว่าการเติมโลหะแกลเลียมสามารถเพิ่มค่าการเลือกเกิดของสารอะโรเมติกส์อย่างมาก
เนื่องจากการเกิดขึ้นของแกลเลียมออกไซด์ไอออนที่ช่วยในการเกิดปฏิกิริยาดีไฮโดรจีเนชัน
(dehydrogenation) นอกจากนี้ผลของความเข้มข้นของเตตระเอทิลออโธซิลิเกตส่งผลเพิ่มขึ้น
เล็กน้อยต่อค่าการเลือกเกิดพาราไซลีนต่อไซลีน ในขณะที่ผลของจำนวนรอบในการเคลือบชั้นซิลิกา
เฉื่อยนั้นส่งผลอย่างมากต่อการเพิ่มค่าการพาราไซลีน เนื่องจากการเพิ่มจำนวนรอบในการเคลือบนั้น
สามารถทำให้เกิดชั้นซิลิกาเฉื่อยที่มีความสม่ำเสมอมากขึ้น ตัวเร่งปฏิกิริยาที่ถูกเคลือบด้วยสารละลาย
เตตระเอทิลออโธซิลิเกต ทำให้ค่าการเปลี่ยนแปลงและค่าการเลือกเกิดสารอะโรเมติกส์ลดลง
เนื่องจากการลดลงของความเป็นกรดบนผิวนอกของตัวเร่งปฏิกิริยา การเติมฟอสฟอรัสด้วยวิธีเติม
แบบเปียกร่วมนั้นส่งผลทำให้เกิดพันธะซิลิโกะอลูมิโนฟอสเฟส โครงสร้างของอะลูมิเนียมแบบใหม่
ชนิดห้าตำแหน่ง รวมไปถึงความเป็นกรดชนิดกลางเพิ่มมากขึ้น ซึ่งมีผลทำให้เพิ่มค่าการเลือกเกิดของ
สารอะโรเมติกส์

GRAPHICAL ABSTRACT

5973022063:   Petroleum Technology Program

Sukkatad Sintapanin: Conversion of *n*-Pentane to Aromatics: Effect of Surface Modification by Chemical Liquid Deposition and Promoter over Nano Scale Ga/HZSM-5

Thesis Advisors: Assoc. Prof. Siriporn Jongpatiwut, 73 pp.

Keywords: Aromatization/ Chemical liquid deposition/ HZSM-5/ *n*-Pentane/ Promoter
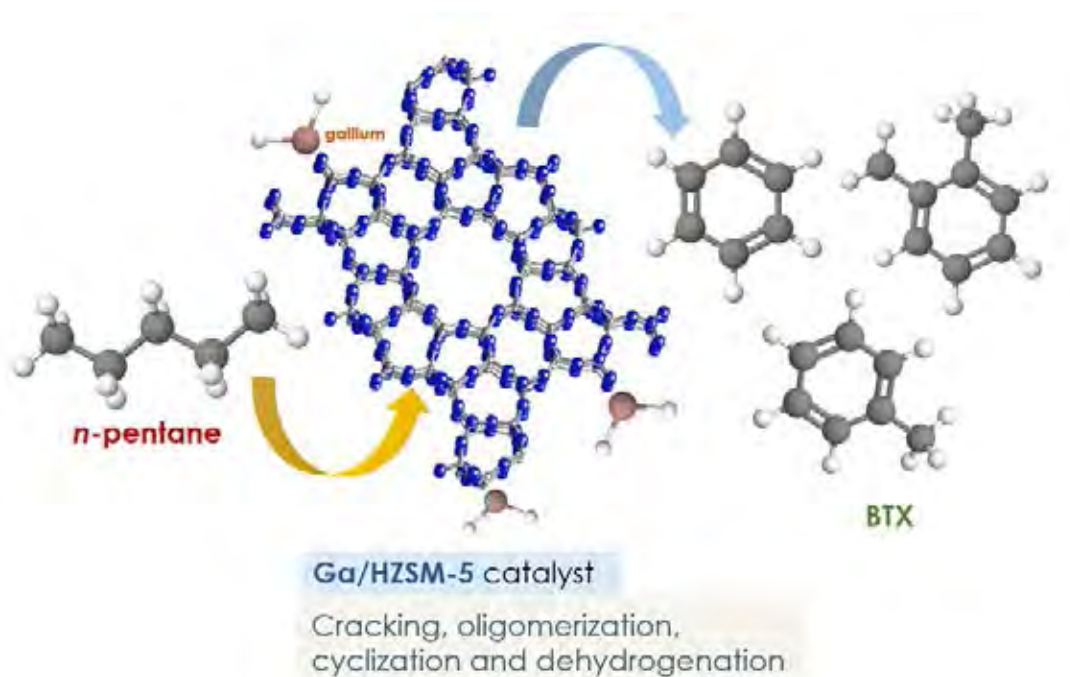
ACKNOWLEDGEMENTS

This work would not have been possible without all the support and the offering of the following people:

I would first like to thank The Petroleum and Petrochemical College for providing the partial scholarship and partial funding of this thesis work including the opportunity to study in Master's degree.

I would like to express my sincere thanks to my thesis advisor, Assoc. Prof. Siriporn Jongpatiwut. She always listens my ideas and help me to solve the problem. Moreover, she taught me not only the knowledge in the research but also the methodologies in my life.

I would like to thank Prof. Pramoch Rangsunvigit for his kind advice, useful guidance, helpful questions, and for being my thesis committee.

I would like to thank Dr. Sitthiphong Pengpanich, who provided me a many discussion, knowledge, materials for this thesis and for being my thesis committee.

I would like to thank my all senior, Mr.Chaninwut Kalajuck and Mr.Thanapon Chuntachat who provided me a testing catalyst preparation, testing catalytic activity, and helped me to solved many problem in laboratory. Moreover, Mrs. Yanika Sa-ngasang who gave me some suggestion.

This thesis work is funded by Center of Excellence on Petrochemicals and Materials Technology (PETROMAT).

Special appreciations go to all of the Petroleum and Petrochemical College's staff who help in various aspects, especially the Research Affairs staff who kindly help with the analytical instruments used in this work.

Special thanks go to my friends at PPC for their kindly help, encouragement, good suggestion, my two years in the College was so meaningful.

Most importantly, all the success things in my life always receive the love, encouragement, and support from my family. I would like to present this thesis to my parents, who have always been the motivation of my life.

TABLE OF CONTENTS

LIST OF TABLES

TABLE   **PAGE**

LIST OF FIGURES

FIGURE **PAGE**

CHAPTER I

INTRODUCTION

The important objective in refinery and petrochemical industry is to increase high value products. Large volume of light paraffin hydrocarbon in market, especially *n*-pentane is come from petroleum refinery processes affecting to high availability and low value of *n*-pentane. Therefore, it is interesting to convert *n*-pentane to more valuable chemical products such as light aromatics (benzene, toluene and xylene known as BTX) . These aromatic compounds are the most important basic raw materials in many chemicals. Aromatics is normally used as additive in refinery to increase the octane number of gasoline. *p*-Xylene is industrially important feedstock because it can be used to produce polyester applying in clothing, plastic and packaging manufacture. Moreover, polyethylene terephthalate is one of the petrochemical products from *p*-xylene that widely used in many advantages such as recyclable soft drink bottle, high UV resistance additive and high durability.

ZSM-5 zeolite or MFI is generally used to convert light alkane to aromatic products which ZSM-5 is crystalline aluminosilicates of AlO_4 and SiO_4 tetrahedral formation in three dimensional frameworks. The reason of using ZSM-5 in alkane aromatization is shape selectivity property of this zeolite suitable to light aromatic compounds. A lot of studies show that the incorporation gallium to ZSM-5 can enhance in the dehydrogenation alkane to produce alkene which affect to other reactions in aromatization e.g. oligomerization, cracking, cyclization (Pidko *et al.*, 2007). Nevertheless, *p*-xylene selectivity from Ga/ZSM-5 is not high enough. So, the modification of Ga/ZSM-5 after synthesis is very interesting. There are many methods to improve the selectivity of aromatics and *p*-xylene. Chemical liquid deposition or CLD can be applied to zeolite for removing the external acid site of ZSM-5. Silylation with tetraethylorthosilicate (TEOS) can enhance the *p*-xylene selectivity by narrowing and blocking the pore opening along with deposition the silica layer on external site of ZSM-5 to prevent the isomerization of *p*-xylene to other isomer forms (Yue *et al.*, 1996).

Moreover, the effect of particle size of ZSM-5 to 1-hexene aromatization was studied by Su and co-workers, they found that nano scale ZSM-5 showed better the catalytic activity because the presence in mesopore had the shorter diffusion path lengths and suppress the coke formation (Su *et al.*, 2017). However, Zheng and co-researchers also found that the chemical liquid deposition with TEOS on the smaller crystal size zeolite had the lower effect than larger size zeolite (Zheng *et al.*, 2003).

In addition, the addition with phosphorous and lanthanum to Zn/HZSM-5 was studied by Long and co-workers. The results indicated that the addition with La and P to Zn/HZSM-5 could promote the aromatics selectivity due to the increasing the $[Zn(OH)]^+$ species which had the effect to convert light olefins into aromatics compound (Long *et al.*, 2014).

This research focuses on the effect of parent nano scale and micro scale ZSM-5 zeolite and combined gallium incorporation and silylation with TEOS in nano scale zeolite. Moreover, the effect of promoter e.g. platinum, phosphorous, zinc, and lanthanum to Ga/ZSM-5 by co-impregnation method is also studied. The modified ZSM-5 will be introduced in *n*-pentane aromatization reaction to maximize the activity of *n*-pentane conversion, aromatic and *p*-xylene selectivity. In addition, the catalysts were characterized by NH_3-TPD, IPA-TPD, TPR, XRD, TPO, NMR and N_2 adsorption.

CHAPTER II
THEORETICAL BACKGROUND AND LITERATURE REVIEW

It is generally known that aromatics have effective importance to human life because it is used to produce many products which relate to daily use such as medicine, telecommunication, cloths and packaging. Moreover, aromatics are the most valuable chemicals in petrochemical industries and refinery due to using these substances as chemical feedstocks, especially benzene, toluene and xylene (BTX). p-Xylene had high demand in global market more than 37 million tons in 2014 and is expected to obtain 63 million tons in 2022. On the other hand, amount of n-pentane is continuously increased in market due to more operation of fluid catalytic cracking including value of n-pentane is low. For these reasons, it is interesting to increase value of n-pentane by converting to aromatic compounds.

2.1 Aromatic Hydrocarbons

Aromatic hydrocarbon is an unsaturated cyclic compound which is consisted of carbon and hydrogen atom. The bonds in aromatic hydrocarbon are sigma bonds and delocalized pi-electrons between carbon atom which provide stability, chemical and physical properties. The term aromatic was assigned because many of aromatic compounds have a sweet or pleasant scent. Benzene is the simplest aromatic hydrocarbon with hexagonal structure and contains three double bonds between carbon-carbon atoms. Aromatic hydrocarbon can be divided into two types. First, monocyclic (MAH) is the compound with only one benzene ring and polycyclic (PAH) contains more than one benzene rings. It is generally known that aromatic hydrocarbons are very important chemical feedstocks to petrochemical industry. Benzene, toluene and xylene (BTX) are important raw feedstocks in the production of polymer, other chemicals and various products (solvent, paints, pharmaceutical) as shown in Figure 2.1.
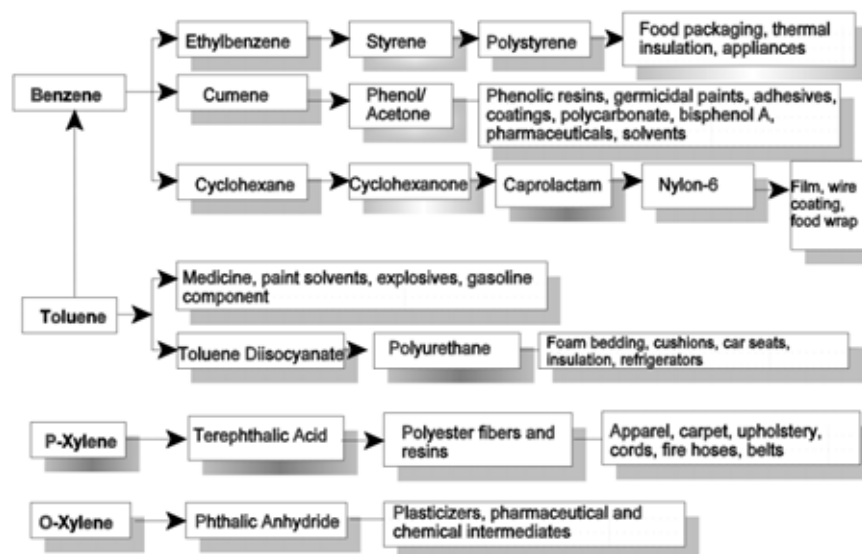
Figure 2.1 The BTX chain.

The BTX production can be made by many processes. Most of them is produced by catalytic reforming of naphtha in refineries. The demand of benzene, toluene and xylene relate to plastic market. Nowadays, the global demand of plastic is very high, especially polyethylene and polypropylene while it affects to low demand for some chemical such as polystyrene and polyvinyl chloride. High capacity production leads to lower demand in exportation from Asia and decreasing prices with margin continue to near term problem for the BTX chemicals. Moreover, the high global demand for polyester fibers, film and bottle resins leads to increase *p*-xylene need and stimulates to build additional production of *p*-xylene. The global *p*-xylene market will be extended to reach USD 66.93 billion in 2022. The research from Grand View show that the high demand of polyester resin and fiber from many industries will be expected to push *p*-xylene market over the predicted period. For example, terephthalic acid is used as the feedstocks to produce polyester, especially in Asia Pacific which motivates the *p*-xylene demand not only the recent past but also continuously grow to seven years. The global demand of *p*-xylene market was higher than 37 million tons in 2014 and expected to achieve 62.98 million tons in 2022.

Xylene or dimethyl benzene is an aromatic compound containing one ring with two methyl groups attach at different substituted positions. There are three form isomers of xylene which depend on relative position of methyl (CH_3) group on the benzene ring. First, *o*-xylene (1,2-dimethylbenzene) indicates the methyl groups are substituted on adjacent, the methyl groups of *m*-xylene (1,3-dimethylbenzene) are substituted on the first and third of benzene while *p*-xylene (1,4-dimethylbenzene) shows the methyl groups on the first and fourth position. Physical properties of *p*-xylene are colorless, flammable liquid or crystal and characteristic odor. Moreover, *p*-xylene can explode if ignited in an enclosed area and there is dangerous hazard form flashback. The isomerization of mixed xylenes as shown in Figure 2.2.

1,2-dimethylbenzene   1,3-dimethylbenzene   1,4-dimethylbenzene
(*ortho*-xylene)   (*meta*-xylene)   (*para*-xylene)
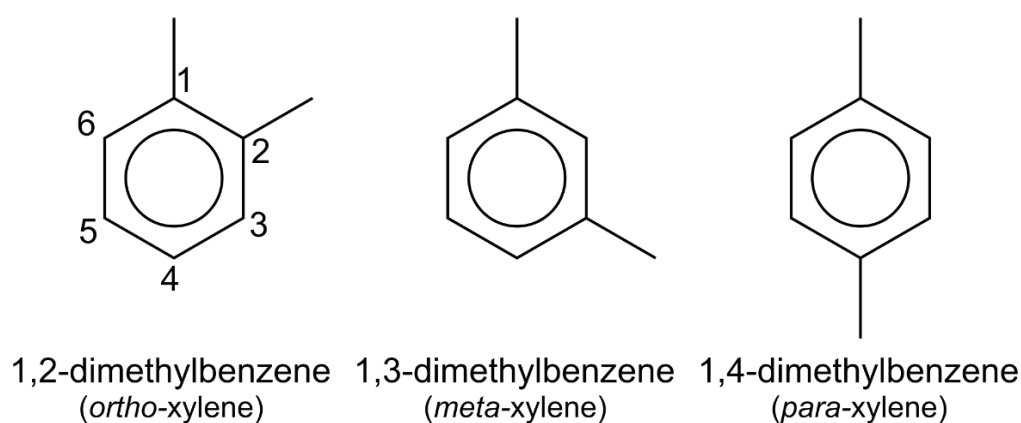
Figure 2.2 The isomerization of mixed xylene.

Most of *p*-xylene production comes from isomerization and separation processes. The isomerization of xylene is restricted by the thermodynamic equilibrium product distribution resulting in 23% of *o*-xylene, 53% of *m*-xylene and 24% for *p*-xylene over shape-selective catalysts such as ZSM-5 zeolite. In addition, there is secondary isomerization of xylene from external acidic affecting to rapidly isomerize of *p*-xylene to the other isomer form, so the selectivity of *p*-xylene production considerably decreases together with increases the separation cost to obtain desired xylene isomers.

In petrochemical industries, there are a large amount of light alkane hydrocarbon (C_2-C_5) form the operating system. Ethane is mostly used to produce

ethylene which are important feedstock in petrochemical and plastic industries while the mixture of propane and butane are used as fuel in many applications. *n*-Pentane is mostly used as additive in gasoline, but it has some disadvantages such as low octane number and high RVP. Therefore, the price of *n*-pentane is low and high supply in market. For these reasons, converting *n*-pentane to high value products especially *p*-xylene becomes interesting.

Zeolites have various structural types, for example, ZSM-5, ZSM-12, modenite, Erionite, etc. The aromatization or dehydrocyclization of alkane over ZSM-5 based catalysts was studied by (SCURRELL, 1988), (Guisnet *et al.*, 1992) and (Viswanadham *et al.*, 1996). For the chemical catalyst, ZSM-5 zeolite is extensively applied in many industrial areas because this zeolite type can prevent the formation of large molecule hydrocarbon and block the coke deposition. Therefore, ZSM-5 can enhance the stability and activity of many reactions in alkane aromatization.

The aromatization reaction of light paraffin includes many reaction networks following.

1) Dehydrogenation and/or cracking of light alkane
2) Oligomerization of olefins and cracking of oligomer
3) Olefin alkylation
4) Cyclization of olefin to naphthene or cycloalkane
5) Dehydrogenation of naphthene to aromatic

Converting alkane to aromatic normally decreased with the increasing silica (SiO_2) to alumina (Al_2O_3) ratio because high SiO_2/Al_2O_3 ratio affect to the decreasing acidity of zeolite. Gao and co-workers found that low SiO_2/Al_2O_3 of ZSM-5 zeolite showed high both acid density and acid strength resulting in higher selectivity of aromatic selectivity (Gao *et al.*, 2016). Moreover, Danuthai and co-woekers studied the aromatization of *n*-octane over ZSM-5 zeolite. The results indicated that the lower SiO_2/Al_2O_3 (Si/Al=10) showed *n*-octane conversion about 99.2% and 25.5% of aromatic selectivity while the higher SiO_2/Al_2O_3 (Si/Al=100) converted only 48.3% of *n*-octane and total aromatic selectivity only 1.7% (Danuthai *et al.*, 2006).

Currently, aromatization processes are generally known in the petrochemical industries. There are many important processes to produce aromatics from light alkanes such as reforming, Cyclar and Alpha process.

2.1.1 Reforming Process or CCR Platforming Process

The reforming process was developed for production aromatics or high octane gasoline from the desulfurized naphtha. This process is operated in very high severe condition to produce high aromatics yield. Heavy naphtha (C7-C9) is important feed in this process using bifunctional catalysts especially, $Pt/Cl-Al_2O_3$ catalyst. In the refinery, the catalytic reformer is used as important unit to provide high value products for example, reformate for the gasoline pool and benzene, toluene and xylene for petrochemical applications. In addition, light naphtha is applied as a feed in this process to produce more valuable high octane gasoline.

Major reactions in the CCR platforming process can be divided in to four parts to produce aromatic products. First, dehydrocyclization of paraffins to 5-membered rings. Next, these rings are isomerized to 6- membered rings and then dehydrogenation 6- membered rings to aromatics. Finally, they will be cracked with hydrogen to smaller hydrocarbons. This process requires little possible in ring opening or cracking. The diagram of CCR platforming process is shown in Figure 2.3.
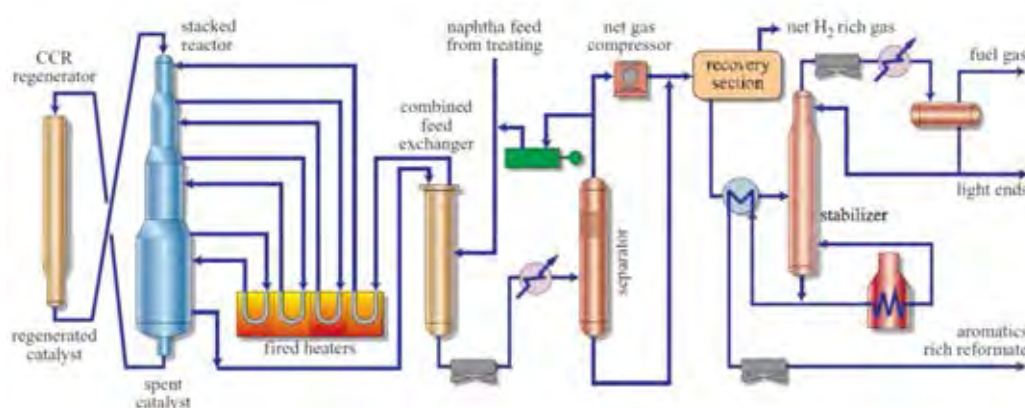
Figure 2.3 Schematic diagram of CCR platforming process.

2.1.2 Cyclar Process

Mixed aromatics are produced in the Cyclar process by using feed as propane and/ or butane together with applying a series of reactions called dehydrocyclodimerization. In the first reaction, the dehydrogenation reaction of paraffin to produce olefins is rate limiting step. After that, the olefins will be rapidly oligomerized to larger intermediates and cyclized to naphthenes. The last step is the dehydrogenation of naphthenes to aromatics. The schematic of the Cyclar process is shown in Figure 2.4 (Perego, 2006).
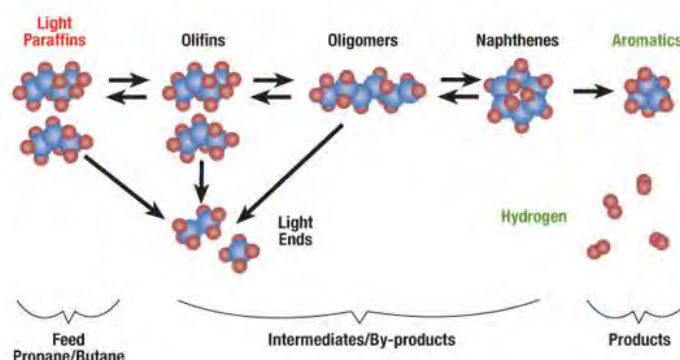
Figure 2.4 Network reaction of the Cyclar process.

The net reactions in this process are endothermic reactions which is thermodynamically favored at temperature higher than 425ºC to complete conversion of reaction and require multiple stages together with reheat between stages obtaining high conversion and maintaining aromatic selectivity. Continuous Catalyst Regeneration (CCR) technology is used in the Cyclar process to remove coke amd undesirable products from the catalytic reaction. For these reasons, it can enhance the stability of reaction in the operation. Mixed aromatic are the main products and hydrogen gas is mostly byproduct. The composition of aromatic products will slightly change in types of feedstocks (pure propane to pure butane and mixtures of these) as the amounts of hydrogen are relatively constant. The mixed aromatics have a very low trace of paraffin. Moreover, benzene, toluene and mixed xylenes can be recovered without an extraction unit. On the other hand, there are many number of stacked moving-bed radial-flow reactors in the Cyclar process and the catalyst is flown to the

bottom of reactors, regenerated and introduced to the top side of reactor. Over the time, coke formation in this process becomes important problem. After the reaction, aromatic products are separated and stripped to get higher purity. The diagram of Cyclar process is shown in Figure 2.5.
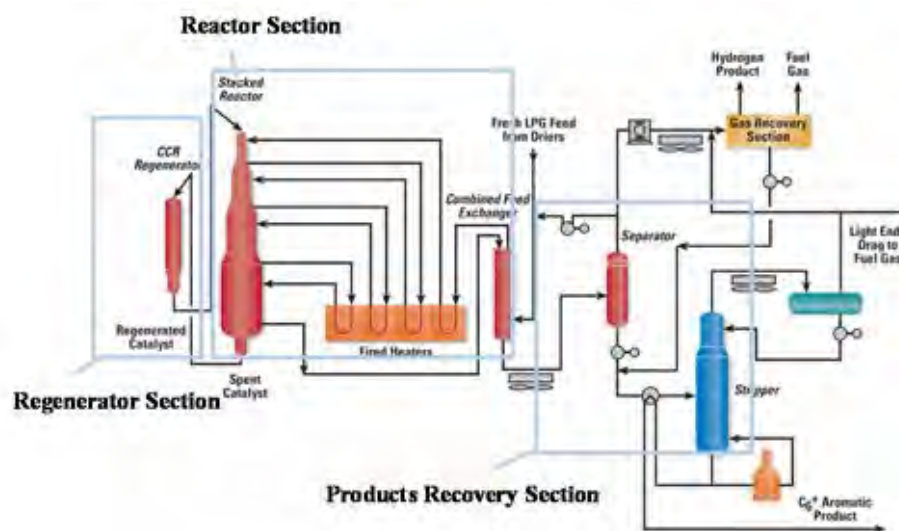
Figure 2.5 The diagram of Cyclar process.

2.1.3 Alpha Process

Alpha process was developed by Sanyo Petrochemical Company and now is licensed by Stone & Webster. $Zn/\gamma\text{-}Al_2O_3/ZSM\text{-}5$ catalyst is used in hydrothermal treatment and feedstocks are C3-C8 olefins. For this operation, the similarity of two fixed-bed reactors are applied in swing mode type. The first reactor is used for reaction while the other one is used for catalytic regeneration which the process flow diagram is shown in Figure 2.6.
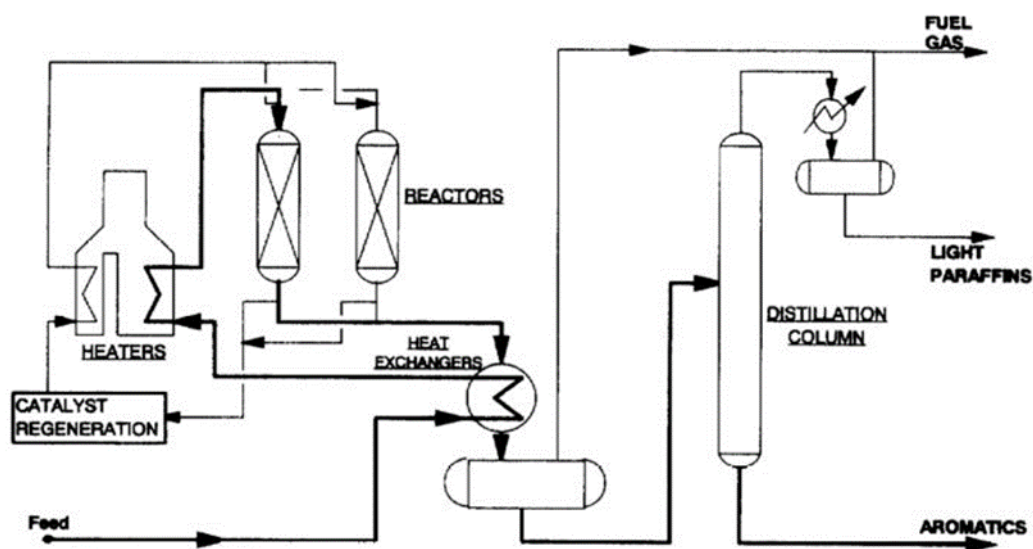
Figure 2.6 The simple process flow diagram in Alpha process.

Coke decomposition in catalysts becomes a major problem to complete the conversion. Therefore, to maintain activity of reaction and the stability of catalyst requires the coke burning that it can enhance the prevention of carbon decomposition.

The coke formation over ZSM-5 zeolite catalyst in these reactions decrease the further efficiency conversion of reaction by strong removal of acid sites which cause prevention the reactants molecule to these acid sites. For these reasons, it is very interesting to control the coke formation over ZSM-5 zeolite but the complete elimination of carbon decomposition is impossible. So, there is some idea to improve the stability by modification catalyst with thermal and hydrothermal pretreatment.

After catalyst regeneration, the result from temperature programmed desorption show that Brønsted acidity of zeolite is diminished significantly to generate Lewis acid site and the framework of Al-OH is suppressed after catalytic regeneration together with reducing in Brønsted acid site (Tagliabue *et al.*, 2004).

2.2 Naphtha Feedstock

Naphtha is an intermediate hydrocarbon which can be obtained from the refinery processed and it can be divided to two types of naphtha. First, light naphtha

mostly contains C_5-C_6 with boiling range is 30-145 °C and heavy naphtha contains at least 6 carbon atoms in structure having boiling in range of 140-205 °C. Naphtha is most usually used in the petrochemical industries for desulfurization and then catalytical reforming. The hydrocarbon molecules in the naphtha are restructured and broken some of the molecules into smaller molecules to produce as additive in octane booster in gasoline. Each refinery produces its own naphtha which depends on the types of crude oils with specific initial boiling points, final boiling points, other physical and compositional characteristics. The naphtha feedstock consists of:

2.2.1 Paraffins or alkanes is an acyclic saturated hydrocarbon. It is generally known that alkanes contain only hydrogen and carbon atoms arranged in a tree structure with single bond of carbon-carbon atom.   The general chemical formula of alkenes is C_nH_{2n+2} and weakly react with ionic and other polar substances. The paraffin density increases with increasing carbon number.

2.2.2 Olefins or light alkenes is an unsaturated hydrocarbon containing at least one double bond between carbon and carbon bonds. The words alkene or olefin are used often interchangeably. Linear alkenes normally contain only one double bond and there are no functional groups known as monoenes. The general formula of alkene is C_nH_{2n}. Moreover, they have the same physical properties with alkanes which are colorless, nonpolar, combustible, and scentless. The physical status of alkenes relates to molecular weight such as the corresponding saturated hydrocarbons. light alkenes such as ethene, propene, and butene are gas state at atmospheric temperature.

2.2.3 Naphthenes or cycloalkanes are cyclic hydrocarbons without double bond in structure that contain at least one ring structure. The C_nH_{2n} is general formula of mononaphthenes same as olefins. Five and six carbon atoms are the most abundant cycloalkane in petroleum industry. The rings can be attached with paraffinic side chains to their structure. Naphthenes have higher boiling point and density compared to paraffin with same carbon atoms.

2.2.4 Aromatics contain at least one polyunsaturated rings or conjugated double bonds. In their structure, benzene rings can be attached with paraffinic side or be coupled with other aromatic rings. Aromatic compounds have higher the boiling points and density than both alkanes and cycloalkanes compared to the same carbon

number. At the beginning, aromatic is used as addictive to boost octane numbers in gasoline.

Naphtha is converted into reformate which mostly is BTX by catalytic reforming. The aromatic products are controlled by thermodynamically equilibrium so improvement product selectivity is using bifunctional zeolitic catalysts to modify properly the zeolite pore opening like BTX molecules (Serra *et al.*, 2005).

2.3 Catalysts in Aromatization of *n*-Alkanes

Converting of light paraffins to aromatics becomes interesting since the high availability of low value petroleum feedstocks especially light naphtha in refineries. Light naphtha is obtained from many units in petrochemical industries and refineries such as fluid catalytic cracking, steam cracking and hydrotreating processes. So, the catalytic conversion of light naphtha is the most relevant challenge in petrochemical both industrial and academic research. It is generally found that the aromatic selectivity is promoted by gallium together with bifunctional catalysts are used as metal oxide of ZSM-5 (Nakamura *et al.*, 1996). Therefore, the conversion of light alkane to aromatics has adopted acid catalysts. The researcher acquires the most of aromatic products through naphtha catalytic reforming. Nevertheless, the aromatic cannot be converted from light hydrocarbons by classical catalysts such as Pt/γ-Al$_2$O$_3$ based catalysts. The shape selectivity and acid properties of ZSM-5 zeolite can applied in aromatization processes by carbon and hydrogen reshuffling in a thermodynamically receptive sense at the relatively low pressure and high temperature condition (Tagliabue *et al.*, 2004). The high aromatic selectivity of MFI or ZSM-5 zeolites is resulted from the similar pore opening size to aromatic molecule and it can be increased by delicate pore opening modification.

2.3.1 Zeolite Materials

Zeolites are crystalline porous aluminosilicate mineral which can be found in nature and they were discovered in 1756 by Swedish mineralogist. The structure of zeolite is represented by regular three dimensional framework form by

tetrahedral, typically SiO_4 and AlO_4, that are linked to each other by sharing oxygen atom at their vertices. The formation of a negative charge in zeolite framework is resulted from the introduction of aluminum atom in pure silica lattice which this negative charge is compensated by extra-framework cations or proton. The chemical formula of zeolites is represented in $M_{2/n}O \cdot Al_2O_3 \cdot ySiO_2 \cdot wH_2O$ where y varies from 2 to infinity, n is the cation valence and w indicates to the number of water molecules confined in the void of the zeolites (Flanigen *et al.*, 2010). The tetrahedral formation of zeolites is referred to T-atoms that primary building units are arranged to yield Si-O-Si and Si-O-Al bonds without formation of Al-O-Al. There are many types of zeolite frameworks which have been presented with unique structure properties. The example of zeolite structure is shown in Figure 2.7.
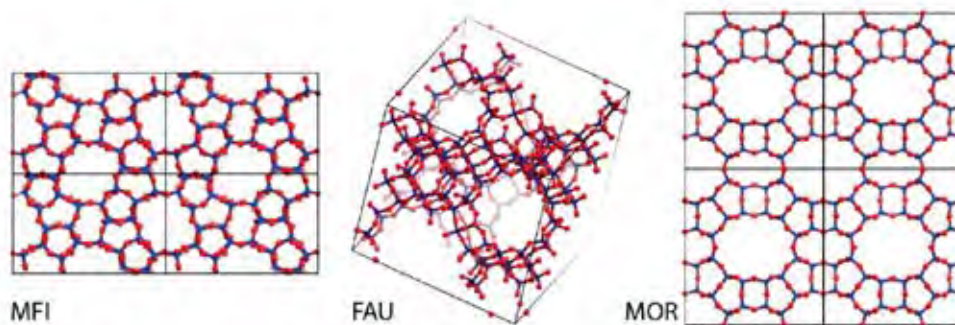
Figure 2.7 Framework structure of MFI, FAU and MOR zeolite.

Zeolites are the most important of catalytic material in petrochemical and refinery processes but only ten types of all known synthetic zeolite are applied in industrial applications. Because the mechanical properties and hydrothermal resistance of most of synthetic zeolites cannot meet requirement for industrial processes. In addition, the cost of development and large scale production of zeolite materials are the highest role. ZSM-5 (MFI), mordenite (MOR), MCM-22 (MWW), β (BEA) and zeolites Y (FAU) are generally used in most of industrial applications such as fluidized catalytic cracking, hydrocracking, reforming, xylene isomerization, alkylation of aromatics etc (Bahatia, 1990).

Zeolitic materials show different types of organic reactions shape activity for example, the reactant selectivity, the reacting molecules can access into zeolite pores. For this reason, product selectivity will be diffused to external of the pores. These reactions will occur due to the fit between the transition state and inside of zeolite pores. Moreover, there is the effect surrounding zeolite on the relative important to the side reactions.

2.3.2 <u>MFI Zeolite (ZSM-5)</u>

The high silica in framework of ZSM-5 type is shown in Figure 2.8, the oxygen atoms link each sheet with the next to form three dimensional structure. For the inversion center, the adjacent sheets are related to one another which the angle between 10 ring of sinusoidal channels form to the sheets in x axis and the straight 10 ring channels form in parallel with the corrugations (along y) is 90º. For IUPAC classification, micropores diameters have ranged from 0.3 to 2 nm., mesopores size around 2 to 50 nm. and higher than 50 nm. for macropores. Generally, ZSM-5 is used in a variety of petrochemical and refinery applications because it shows the most complex types of zeolite framework which 12 T-atoms are contained in the asymmetric unit.
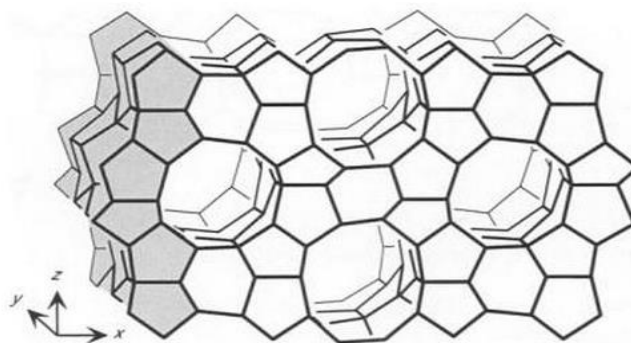
Figure 2.8 The structure of MFI framework type.

2.3.3 <u>Zeolite Framework Type</u>

The structures of zeolite framework are basic knowledge for zeolite chemistry perception and the framework type is contrary to the framework structure. These framework structures are represented in the tetrahedral coordinated atom (T-atoms) which relate to the highest potential of symmetry framework (Jacobs *et al.*, 2001). The three letter code (e.g. MFI, FAU) of zeolite is defined for framework types depending on the observed symmetry, composition in framework and real dimensions of unit cell by the Structure Commission of the International Nomenclature. It is generally known that the code will be obtained from the type material name of zeolite, for example MFI from ZSM-5 (Zeolite Cocony Mobil-five). ZSM-5 allude to a medium pore with channel being referred to the more favorable ten member rings to the diffusion of *p*-xylene among other isomers.

2.3.3.1 Sorption of Molecule with Varying Kinetic Diameter

To evaluate the distribution of micropore size, the most direct method is to make the comparison between the molecule sorption isotherms with minimum various kinetic diameters. The exploration in uptake of sorbates' series along with the growing minimal kinetic diameter on a solid state. The amount of absorption drops with increasing of the sorbate size refers to the least pore diameter of the tested solid. Figure 2.9 shows the comparison between different molecules minimum kinetic diameter and the zeolite pore size diameter.
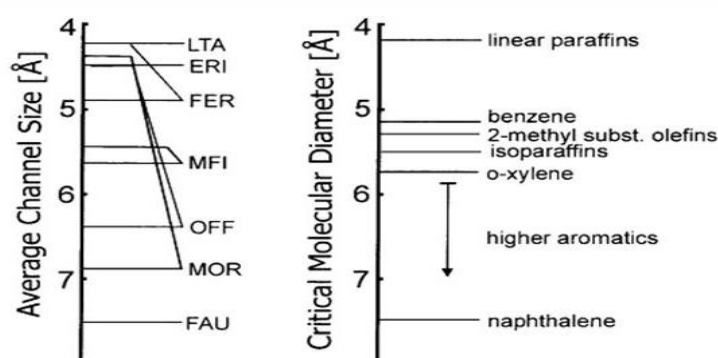
Figure 2.9 Pore diameters of zeolites and sizes of reactant molecules.

In the existence of various functional groups, the sites fraction evaluation which are located at internal or external to the microporous material particles can be used by spectroscopy. The natural limitation of pore sizes is defined to vapor pressure and size of sorbate. The adsorbed molecules in microporous can be stably observe lattice and alterations in the effective material of pore diameter leading to the strong temperature with accessible dependence.

2.3.3.2 Framework Composition

Most of studying in zeolite's properties is based on their negative charge framework which exchange with positive charge for balance ion. The silica (SiO_2) composition in zeolite shows the neutral framework charge but when trivalent of Al atom replaces to the tetravalent of Si in an aluminosilicate production, the framework charge of zeolite will become negative which is required its charge compensation with exchangeable cations such as Na^+, K^+, Mg^{2+}, etc. These positive ions are loosely fixed in zeolite channels and they can be replaced by contact solution or other chemical treatments. The addition small amount of a transition element to zeolite framework is the useful material modification in catalyst. Nowadays, various elements are used to incorporate into zeolite framework such as Pt, Ni, Zn, Ga, etc (Serra *et al.*, 2005). This modification in zeolite framework composition affect to stability of material. Generally, zeolite with high silica will perform a higher thermal resistance compared to the corresponding aluminosilicate. The acidic strength and acidic site of ZSM-5 are effect from the silica to alumina ratio framework. Table2.1 shows the properties of zeolites categorized by their Si/Al ratio (Gates, 1992).

Table 2.1 Acid properties of zeolites classified by Si/Al ratio

Si/Al atomic ratio	Zeolites	Properties
Low (1-1.5)	A, X	Relatively low stability in framework; low stability in acidity; high stability in basicity; high concentration of acid groups with concentration of acid groups with moderate acidity
Intermediate (2-5)	Erionite Chabazite Clinoptilolite Mordenite Y	Relatively low framework stability; low stability towards acid; low stability towards base; medium to high concentration of acid groups with high acid strength in case of Si/Al ratio higher than 2.5
High ($\sim$ 10- ∞)	ZSM-5 Erionite[b] Mordenite[b] Y[b]	Relatively high framework stability; high stability in acidity; low stability in basicity; low concentration of acid groups with high acid strength

Y[b] is zeolite form modified with chemical framework (dealumination).

2.3.3.3 Extra-Framework Species

The channels and cages in zeolite framework are normally placed with extra-framework species for example, the exchangeable positive charge which compensate the framework negative charge, removable water molecules or other organic compounds. These results can be come from the mixture during synthesis process or post synthesis treatment. Modern method in crystallographic approve for the information extraction from the diffraction data. However, there is some limitation in this technique. The primary problem results from the fact that the extra-framework does not follow in the high framework zeolite, so these will refer to disorder.

Catalytic activity of zeolite is essentially affected by the reactive component and transportation of local sites electron in zeolite framework. In

Table 2. 2, the acid-based sites of zeolite are generally Brønsted acid sites which localize H^+ ion near to a Si-O-Al cluster bridging.

Table 2.2 Acid and base systems of zeolite

System	Acid	Base
Arrhenius	Form H^+	Form OH^-
Brønsted-Lowry	Donate H^+	Accept H^+
Solvent	Cation(+)	Anion(-)
Lewis	Accept electron pair	Donate electron pair

The Brønsted acid sites from ZSM-5 zeolite catalyst are related to aluminum located in zeolite framework while the extra-framework aluminum correlate to Lewis acid sites.

2.3.3.4 Deactivation of Catalyst

There is specific lifetime of zeolite catalysts in diverse structure. Catalyst deactivation mainly happens from the coke decomposition. Normally, three-dimensional type of zeolite's structure can be deactivated by a lesser rapidly given amount of coke compared to one-dimensional framework type. Blocked channel at one point in three-dimensional zeolite still be used for the catalytic reaction through interconnections.

2.4 Modification of Zeolite

The good activity and light alkane conversion to aromatic selectivity are result from monofuctional acid catalyst in ZSM-5 structure. Nevertheless, it still not be the best dehydrogenation catalyst directing toward the limitation in aromatic selectivity due to removable hydrogen from catalyst which occurs by hydrogen transfer to olefins. Aromatization over ZSM-5 is accompanied by the C-C alkane bond cracking with three moles of small alkanes production to form one mole of aromatics (Asaftei *et al.*, 2009). In addition, there are many limitations in aromatics formation

over ZSM-5. First, thermodynamic equilibrium data of conversion alkane to aromatics is more difficult than using alkene as feedstock. Second, the alkane aromatization kinetic is limited by olefinic compound formation taking place hydrogen and carbenium ions from carbonuim ions scission. The next step is formation of aromatics occurring to the transferring of hydride from cycloalkane or naphthenes into smaller olefins. Finally, the pore structure in ZSM-5 limit the transferring hydrogen to olefinic compounds from naphthenes. Accordingly, the modification ZSM-5 is desired to improve the properties that lead to increase conversion and shape selectivity to paraxylene. It has been studied many modification methods in ZSM-5 e. g. dealumination, metal incorporation, chemical liquid decomposition (silylation) with silica compounds and subsequent reduction oxidation treatment.

2.4.1 Metal Incorporation

Most of processes for metal incorporation is done in engineering field. The study on conversion of light alkane to aromatics is done to understand the effect of metal ions in aromatization process. The incorporation of platinum, zinc and galliun on ZSM-5 has an influence in pentane aromatization because high aromatic selectivity can be promoted by the increasing in alkanes dehydrogenation (Meriaudeau *et al.*, 1991). The effect of incorporate nickel to ZSM-5 zeolites in *n*-pentane aromatization was studied by Ihm and co-researchers. They found that Ni/ZSM-5 can promote activity in *n*-pentane aromatization due to the increasing Lewis acid sites and Ni^{2+} has the effect to convert olefin intermediate to aromatics (Ihm *et al.*, 1994).

The effect of boron modification of ZSM-5 in fast pyrolysis of cellulose to aromatic was studied by Zhou and co-researchers. They found that the impregnation 1 wt% boron with ZSM-5 zeolites preserves the monoaromatic hydrocarbons and decrease undesired products because boron can reduce the pore size of ZSM-5 and penetrates into the channels and bound with acid strength of ZSM-5. In addition, the deposition of boron to ZSM-5 affects to pore narrowing which enhances the *p*-xylene selectivity over *m*-xylene and *o*-xylene (Zhou *et al.*, 2014).

Ga ion-exchange with HZSM-5, Ga/ZSM-5, shows the higher aromatics yield and selectivity in aromatization of *n*-pentane compared to no modification over HZSM-5. The presence of Ga^{3+} ion in ZSM-5 can enhance the lower

olefin conversion to aromatics but it does not affect to acid property and the cracking ability in zeolite (Sirokman *et al.*, 1986).

The effect of Ga/ZSM-5 on propane aromatization which influences on time-on-stream was studied by Choudhary and co-workers. It was found that the strong acid sites of zeolite reduce due to increasing amount of Gallium loading which proton in zeolite framework is replaced by gallium ionic species e.g. Ga^{3+} or GaO^+. Moreover, the effect of increasing Gallium loading is more coke formation on zeolite when increase time-on-stream because of the promotion dehydrogenation activity to catalyst presented by the Gallium oxide species in zeolite channels. Moreover, they found that gallium loading 3 wt% in zeolite enhances the *p*-xylene selectivity (Choudhary *et al.*, 2000).

Fujimoto and co-workers studied the effect of gallium and platinum over ZSM-5 in butane aromatization. The result indicates that Ga/ZSM-5 exhibits a good performance in aromatic selectivity due to the attribution in dehydrogenation or dehydroaromatization of olefins while the incorporation platinum to ZSM-5 slightly promotes the aromatic selectivity and suppresses small olefins formation (Nakamura *et al.*, 1996).

The co-impregnation with lanthanum and phosphorous to Zn/ZSM-5 in upgrading FCC to aromatics compounds was studied by Long and co-workers. They found that the introducing La and P to Zn/ZSM-5 could promote the aromatics selectivity due to the increasing of [Zn(OH)]+ which affected to convert olefins to aromatic compounds (Long *et al.*, 2014).

2.4.2 Silylation of HZSM-5

Silylation is the one method among a variety of improvement zeolite to increase the *p*-xylene selectivity which this method uses the inert silica layer to deposit on external surface of ZSM-5. Chemical vapor decomposition (CVD) or Chemical liquid decomposition (CLD) is common method to sylilate zeolite that effectively increases the *p*-xylene selectivity to eliminate external acid site of zeolite with adjust pore mouth of ZSM-5. The CVD method is hard to operate because of the shortage of reproducibility comparing to CLD has significant effect to apply in industries. CLD

process requires solvent to carry the gradual CLD agent diffusion through on zeolite surface that lead to the more effective silylation at the less deposition agent amount.

Zheng and co-workers studied the effect of CLD to improve p-xylene selectivity which the diffusion process is controlled by narrow pore mouth in pore-opening. Small crystalline size of ZSM-5 has more acid strength at external surface and area of pore mouth compared to the large size of crystal. Briefly, the big crystal size CLD largely affect in silylation due to the lower acidity (Zheng et $al.$, 2006). Teng and co-worker studied the effect of CLD agent affecting to shape selectivity on modified ZSM-5. Tetraethyl orthosilicate (TEOS) is the best solvent in silylation among dimethyl silicone (DMS), phenylmethyl silicone (PMS), and hexamethyl disiloxane (HMDS) because TEOS has the lowest viscosity which easily leads silica layer to uniform. The diameter of TEOS is 1.03 nm which larger than micropore opening of ZSM-5 zeolite while hydroxyl groups in external surface close to the pore opening that Si-O-Si or Si-O-Al can be formed due to the reacting between deposition agent and this functional groups. However, this result might affect to deactivation of non-selective acidic sites from outer surface (Teng et $al.$, 2011).

The effect of different crystal size on modified ZSM-5 by chemical liquid deposition was studied by Zheng and co-researchers. They used different particle size ZSM-5 in toluene disproportionation. The result showed that this modification have more effective in the larger crystal size zeolite at the same silylation level. Moreover, they found that multicycle silylation is required to narrow the pore mouth and deactivate the external acid sites of small crystal size zeolite to improve the p-xylene selectivity (Zheng et $al.$, 2003).

By the way, Nitipan and co-workers studied the effect of metal ion exchange and silylation on the conversion light alkanes to aromatic over the ZSM-5 zeolite and influence of TOES loading together with different concentrations of TEOS in the unification on Ga/ZSM-5 catalyst. The result in this combination can rapidly promote the p-xylene selectivity which the highest p-xylene selectivity can reach to 99.7% with 20 vol% of TEOS loading. On the other hand, the increasing concentration of TEOS leads to lessen n-pentane conversion because the deactivation on the external acid site and surface area reduction of surface areas affecting to m-xylene and o-xylene

diffusion. For these reasons, *p*-xylene formation is transformed from isomerization of both *m*-xylene and *o*-xylene which prior the escaping pores (Nitipan *et al.*, 2012).

    2.4.3 <u>Dealumination</u>

ZSM-5 zeolite is commonly applied in many applications because of its good catalytic properties e.g. shape selectivity, medium pore size, higher stability in coke formation compared to other types of commercial zeolite. Removal acid site or blocking reactant molecules to catalyst is caused by coke decomposition over ZSM-5 catalyst. Therefore, it is very interesting to control location of coke formation in the industry. Aukett and co-workers studied the state of aluminium in ZSM-5 by partial rearrangement aluminosilicate framework. Dealumination process accommodate by the presence of water molecules that the positive charge site of AlO^+ species will be partly neutralized by electron transfer from these hydroxyl group in water molecules. Moreover, the generated AlO^+ species in the steaming of zeolites show the increasing in Lewis acidity together with the lessening the number of Brønsted acidity (Aukett *et al.*, 1986).

2.4.3.1 Dealumination by Acid Treatment

The definition of dealumination is removing aluminum atom from zeolite framework without damaging the micropore structure which this method is the most widely used to modify catalyst. In this process, only aluminum can be removed form framework but not include the removal extra-framework aluminum or crystallite.

The effect of dealumination was studied by Muller and co-workers showing that the dealuminated ZSM-5 can maintain the structure from the result by XRD (Muller *et al.*, 2000). In addition, Teng and co-workers studied the effect of dealumination by using oxalic acid as agent together with CLD on ZSM. The result in toluene disproportionation show that this modification can increase both conversion and *p*-xylene selectivity (Teng *et al.*, 2011).

2.4.3.2 Dealumination by Steaming Treatment

The study in effect of steaming to acidity on ZSM-5 and aromatization activity was proceeded by Lucas and co-workers. The result shows that initial aromatization activity decreases when increasing the temperature in steaming

pretreatment. Moreover, the stability of dealuminated ZSM-5 by various $WHSV^{-1}$ and temperature show that the high $WHSV^{-1}$ has low stability and easily deactivate from coke decomposition than lower $WHSV^{-1}$. For 550 ℃ in steaming and 0.5 h $WHSV^{-1}$ present the best aromatization while the aromatic selectivity decreases after 5 hour due to the weakness of new active sites leading to lower coke formation resistance (Lucas *et al.*, 1997).

2.4.4 Particle Size of Zeolite

The effect of particle size of zeolites shows the important effect in zeolite's properties and also has influence to the performance in their use. The reduction of particle size in zeolite from micro scale to the nano scale shows the increase of the external surface areas and leads to more active sites.

The nano-sized zeolite contains more pore volume and surface area compare to micro-sized zeolites which significantly promoted the presence of mesopore and macropore. Although the main reaction of aromatization is required in micropore, the molecular diffusion can be increased by the mesopore and macropore. Viswanadham and co-workers studied the effect of micro sized ZSM5 and smaller sized ZSM-5 in acetone to gasoline reaction. The result showed that nano sized ZSM-5 reaches the aromatic yield around 69% compared to micro-sized ZSM-5. They also found that the main reason for changing in aromatic yield is resulting from difference in porosity of zeolites. The nano scale ZSM-5 reduced the diffusion path length of molecules in the channels which affects from the presence of larger pore than micropore in catalyst (Viswanadham *et al.*, 2013).

The effect of particle size and acidity of Zn modified ZSM-5 in 1-hexene aromatization was studied by Su and co-workers. They found that microscale ZSM-5 shows the better catalytic activity resulting from smaller particle size, weaker in acid strength and shorter diffusion path lengths. These reasons improved the formation of aromatics and suppresses the coke formation (Su *et al.*, 2017).

CHAPTER III
EXPERIMENTAL

3.1 Materials and Equipment

3.1.1 Feedstock

- *n*-Pentane 99 % purity was obtained from RCI Labscan Limited.

3.1.2 Gases

- The ultra-high purity (UHP) hydrogen was used for aromatization of light hydrocarbon testing, and for FID detector.
- The high purity (HP) helium was used for purging catalysts after reaction testing and carrier gas.
- The zero grade air was used for FID detector.
- The high purity (HP) nitrogen for TCD detector.
- The 5 vol. % oxygen balanced in helium was used for the temperature-programmed oxidation (TPO) measurement.
- The 5 vol % hydrogen balanced in argon was used for the temperature-programmed reduction (TPR) measurement.

    All gases mentioned above are supplied from Linde, Thailand.

3.1.3 Chemicals

- The commercial nano scale ZSM-5 zeolite (SiO_2/Al_2O_3 = 25) are obtained from PTTGC, Thailand.
- *n*-Pentane of 99% purity are obtained from RCI Labscan, Thailand.
- Light naphtha (C_5-C_6) are obtained from PTTGC.
- Gallium(III) nitrate hydrate ($Ga(NO_3)_3.xH_2O$) is obtained from Aldrich, USA.
- Hexachloroplatinic acid (H_2PtCl_6) is obtained from Aldrich, USA
- Lanthanum(III) nitrate hexahydrate ($La(NO_3)_3.6H_2O$) is obtained from Aldrich, USA.

- Zinc(II) nitrate ($Zn(NO_3)_2.6H_2O$) is obtained from Ajax Finechem, Australia.

- Diammonium hydrogen phosphate ($(NH_4)_2HPO_4$ is obtained from Ajax Finechem, Australia

- Tetraethyl orthosilicate ($SiC_8H_{20}O_4$) is obtained from Aldrich, USA.

- Cyclohexane is obtained from Labscan, Thailand.

3.1.4 Equipment

- Catalytic testing system consisting of gas cylinders, mass flow controller (Aalborg-AGFC171S), furnace, and 0.5 ″ O.D. x 19.5 ″ long Pyrex reactor.

- Rigaku X-ray diffractometer.

- Thermo Finnigan sorptomatic, 1100 series.

- Thermo Finnigan modeled TPDRO 1900.

- Temperature programmed reduction (TPR) apparatus.

- Temperature programmed oxidation (TPO) apparatus.

- Shimadzu GC-17A gas chromatograph equipped with a capillary HP-PLOT/Al_2O_3 "S" deactivated column.

- Agilent Model 6890N gas chromatograph equipped with a capillary Stabilwax column.

- Hamilton Syringe pump.

3.2 Methodology

3.2.1 Catalyst Preparation

3.2.1.1 Incipient Wetness Impregnation

The parent nano scale HZSM-5 was impregnated by 1.2 mL solution of precursor ($Ga(NO_3)_3.xH_2O$) equivalent to 1 wt% metal per gram zeolite dried at 110 °C overnight and then calcined with air at 550 °C for 5 h. The modified catalysts were denoted Ga/HZSM-5.

3.2.1.2 Ion exchange

The parent nano scale HZSM-5 was ion-exchanged with 100 mL aqueous solutions containing precursor ($Ga(NO_3)_3.xH_2O$) equivalent to 1 wt% metal in zeolite, stirred for 12 h at 80 °C, washed with excess distilled water, dried at 110 °C overnight and then calcined with air at 550 °C for 5 h. The modified catalysts were noted as Ga/HZSM-5 (IE).

3.2.1.3 Silylation

Ga/HZSM-5(IWI) catalysts were silylated by using chemical liquid deposition method by impregnating the Ga/HZSM-5 with 20, 30 and 50 %vol TEOS in cyclohexane at room temperature for 12 h per gram catalysts, dried at 110 °C for 2 h and calcined at 550 °C for 5 h. The modified catalysts were noted as 20CLD/Ga /HZSM-5, 30CLD/Ga/HZSM-5 and 50CLD/Ga/HZSM-5. The multicycle silylation

3.2.1.4 Multicycle Silylation

30CLD/Ga/HZSM-5 catalysts were silylated for two and three cycles by impregnating with 30 %vol TEOS in cyclehexane at room temperature for 12 h per gram catalysts, dried at 110 °C and calcined at 550 °C for 5 h. The modified catalysts were noted as 2C/30CLD/Ga/HZSM-5 and 3C/30CLD/Ga/HZSM-5.

3.2.1.2 Co-impregnation

The parent nano scale HZSM-5 was impregnated by 1.2 mL solution of precursor ($Ga(NO_3)_3.xH_2O$) equivalent to 1 wt% metal with precursor H_2PtCl_6, $La(NO_3)_3.6H_2O$, $Zn(NO_3)_2.6H_2O$, and $(NH_4)_2HPO_4$ equivalent to 0.2 wt% metal per gram zeolite dried at 110 °C overnight and then calcined with air at 550 °C for 5 h. The modified catalysts were denoted 0.2PtGa/HZSM-5, 0.2LaGa/HZSM-5, 0.2ZnGa/HZSM-5 and 0.2PGa/HZSM-5.

3.2.2 Catalytic Activity Testing

The *n*-pentane aromatization is introduced at atmospheric pressure with continuous flow fixed-bed reactor. In the continuous-flow reactor, catalyst with 0.2 g was used in each run. Prior to aromatization reaction, the modified catalyst was reduced with H_2 at 500 ºC for 2 h. The *n*-pentane feed was continuously fed with a syringe pump and preheated at 70 ºC with flow rate 1.587 mL/h. Nitrogen was used as a carried gas with flow rate 22 mL min^{-1}, WHSV= 5 h^{-1}, reaction temperatures at 500

ºC. The gas chromatography using a Shimadzu 17A-GC was used to analyze products using a Shimadzu 17A-GC equipped with an HP-PLOT/Al$_2$O$_3$ "S" deactivated capillary column. The GC column temperature was programmed to obtain an adequate separation of the products. The temperature was first kept constant at 40 ºC for 10 min and then, linearly ramped to 195 ºC and held for 30 min.

The conversion of feed and selectivity is defined as follows;

$$\text{Conversion (\%)} = \frac{\text{wt. of feed converted}}{\text{wt. of } n\text{-pentane}} \times 100$$

$$\text{Selectivity to product i (\%)} = \frac{\text{wt. of product i}}{\text{Total wt. of products}} \times 100$$

$$p\text{-Xylene selectivity in xylenes (\%)} = \frac{p\text{-xylene}}{p\text{-xylene} + m\text{-xylene} + o\text{-xylene}} \times 100$$
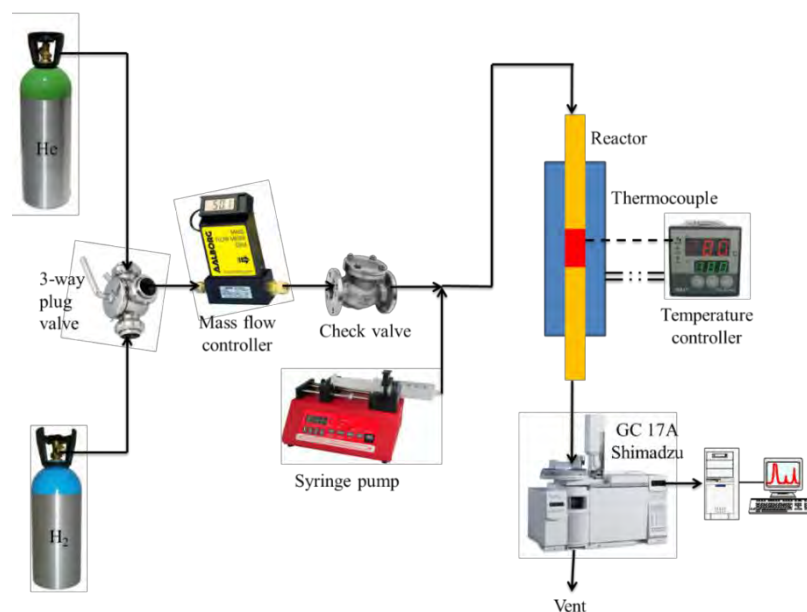
Figure 3.1 Schematic of the experimental set-up for aromatization of naphtha.

3.2.3 Catalyst Characterization

3.2.3.1 Temperature Programmed Reduction (TPR)

This technique was used to determine the reducibility of samples. Temperature programmed reduction (TPR) was performed on the fresh calcined catalysts. For each run, 0.05 g of sample was packed in a 0.25 ″ O.D quartz tube reactor. TPR runs were conducted using a heating rate of 10 °C/min in 30 mL/min flow rate of 5% H_2/Ar and heated to 800 °C.

3.2.3.2 Temperature Programmed Oxidation (TPO)

This technique was employed to analyze carbon deposition over the catalysts during reaction. TPO of the spent catalysts was performed in a continuous flow of 2% O_2 in He while the temperature was heated to 800 °C with a ramp rate of 10 °C/min. The oxidation was conducted in a 0.25 ″ quartz tube fixed-bed reactor. Before the testing, the spent catalyst was dried at 110 °C overnight, weighted (10 mg), and placed between two layers of quartz wool inside the quartz tube. The sample was further purged at room temperature with 2% O_2 in He for 30 min before starting the characterization. The CO_2 being a main product by the oxidation of the coke species was converted to methane in a separation by methanizer which was filled with 15% Ni/Al_2O_3 at 415 °C. The FID detector was used to analyze methane.

3.2.3.3 Temperature Programmed Desorption (TPD) of IPA

The Brønsted acid site of parent HZSM-5 and modified catalysts was tested by the desorption of isopropylamine (IPA). First, 50 mg of sample was pretreated at 500 °C in a flow of He for 1 h. After that, it was cooled in He to 30 °C and then 5 μL pulses of isopropylamine were introduced to the sample, until the sample was saturated. The mass spectrometry was used to confirm saturation of isopropylamine adsorption. After removing the excess of isopropylamine by flowing He for 30 min, the sample was linearly heated with the ramp rate of 10 °C/min to 800 °C. The determining of isopropylamine was monitored by MS signal of 41. The amount of Brønsted site was determined by the amount of propylene observed which was calibrated by pure propylene.

3.2.3.4 Temperature Programmed Desorption (TPD) of Ammonia

The acidity of HZSM-5 and modified catalysts was determined by the desorption of ammonia (NH_3) technique. First, 50 mg of sample was pretreated at 500 °C in a flow of He for 1 h. Then, the sample was cooled in He to 30 °C and then adsorption of ammonia in helium were carried out over the sample, until the sample was saturated. The mass spectrometry (MKS Cirrus) was used to determine the saturation of ammonia adsorption. After removing the excess of ammonia by flowing He for 30 min, the sample was heated to 800 °C with ramp rate of 10 °C/min. The MS signal of 17 were monitored to determine the evolution of ammonia. The amount of acid site was determined by the amount of ammonnia observed which was calibrated by pure ammonia.

3.2.3.5 N_2 Adsorption/Desorption Measurement

The textural properties such as surface area, total pore volume, micropore volume, and mesopore volume of the catalysts were determined by using BET method on a Quantachrom/Autosorb 1-MP instrument. Firstly, the humidity and volatile adsorbents adsorbed on surface of catalyst were removed by outgassing at 300 °C for 12 h. before the analysis step. Next, N_2 was purged to adsorb on surface. The quantity of gas adsorbed onto or desorbed from their solid surface at some equilibrium vapor pressure by static volumetric method will be measured. The solid sample with constant temperature of the sample cell was maintained until reach to equilibrium. This volume-pressure data was used to calculate the BET surface area.

3.2.3.6 X-ray Diffraction (XRD)

The relative crystallinities of the ZSM-5 zeolite and modified ZSM-5 were analyzed by a Rigaku X-ray diffractometer with Cu tube for generating CuKα radiation (λ= 1.5418 Å) at room temperature. The X-ray beam hits a sample and is diffracted to measure the distances between the planes of the atoms. Bragg's Law is: nλ =2d sinθ, where the integer n is the order of the diffracted beam, is the wavelength of the incident X-ray beam, d is the distance between adjacent planes of atoms which is d-spacings and θ is the angle of incidence of the X-ray beam. Since we know, and we can measure, we can calculate the d-spacings. The geometry of an XRD unit is designed to accommodate this measurement. The characteristic set of d-spacings generated from a typical X-ray scan represents a unique pattern of materials.

3.2.3.7 Scanning Electron Microscope (SEM)

This technique is used to determine the morphology of the ZSM-5 zeolite and silylated ZSM-5. The samples were introduced on the stub and coated with a thin layer of platinum. The electrons interact with atoms in the sample, producing various signals that contain information about the sample's surface topography and composition. The electron beam is generally scanned in a raster scan pattern, and the beam's position is combined with the detected signal to produce an image. The SEM images of the catalysts were obtained from a JEOL 5200-2AE scanning electron microscope including with energy dispersive X-ray spectrometer.

3.2.3.8 ^{27}Al MAS NMR Spectroscopy

The samples were hydrated at least for 48 h. and using Al(NO$_3$)$_3$•9H$_2$O as the reference. An excitation pulse with 7 dB power level and a length of 0.6 μs was used with 1D spectrum that had about 250 ms. Relaxation time with the record of 2400 scans. For the ^{27}Al MAS NMR Spectra quantification, the chemical shift and the coupling constant from quadrupolar were obtained from the MQMAS spectrum and adopted for 1D spectra deconvoluting. Demonstration was made for all aluminum types take place in zeolites with coupling constants quadrupole will be detected by above 17.25 T NMR field strengths in correspond to more than 750 MHz. of resonance frequencies. The limitations on the tool at 500 MHz in this work restricted for all (broad) signal contributions resolving. In typical, this fraction of highly distorted aluminum oxygen moieties has been named as "invisible" aluminum extra-framework in which being assessed by the mass balance aluminum.

CHAPTER IV
RESULTS AND DISCUSSION

The aim of this work is to study the effect of chemical liquid deposition of TEOS and promoter in gallium modified HZSM-5 nano scale for its catalytic performance in the conversion of n-pentane aromatization to maximize the activity of n-pentane conversion, aromatics and p-xylene selectivity.

4.1 Catalyst Characterization

4.1.1 <u>BET Analysis</u>

The surface area and pore volume of the parent nano scale HZSM-5 and micro scale HZSM-5 are summarized in Table 4.1. The micropore volume of parent nano scale and micro scale HZSM-5 were approximately 0.13-0.14 cm^3 g^{-1} which is similar to MFI zeolites (Su *et al.*, 2017). The pore size distributions of nano scale and micro scale HZSM-5 are shown in Figure 4.1. The parent nano scale HZSM-5 presented more mesopore and macropore volume than the micro scale HZSM-5 due to the inter-particle voids of nano-particle during formation of crystallinity processes (Viswanadham *et al.*, 2009). After the incorporation of gallium to the nano scale zeolites by impregnation, surface areas, micropore surface areas, and micropore volume decreased resulting from the deposition of extra-framework gallium species to zeolite (Xiao *et al.*, 2015). The mesopore volumes of Ga/HZSM-5 was also increased due to the formation of Ga$_2$O$_3$ during impregnation. The ion exchanged Ga/HZSM-5 surface areas increased because of the replacement of gallium to zeolite framework (Nor *et al.*, 2003). Moreover, the silylation of TEOS on Ga/HZSM-5 led to the decrease of surface areas, external surface areas, and total pore volume due to the deposition of inert silica layer over on external surface of HZSM-5. The addition of promoter did not significantly change to textural properties compared to Ga/HZSM-5, except 0.2ZnGa/HZSM-5 showed the decrease in surface areas due to ZnO which located on external surface and block micropore (Lai *et al.*, 2016).

Table 4.1 BET surface area, micropore surface area, total pore volume, micropore and mesopore volume of the parent nano scale, micro scale and modified HZSM-5 zeolite catalysts

Catalyst	Surface area (m^2/g)	Micropore surface area (m^2/g)	Total pore volume (cc/g)	Micropore volume (cc/g)	Mesopore volume (cc/g)
Parent Nano HZSM-5	381	290	0.513	0.154	0.359
Parent Micro HZSM-5	351	247	0.259	0.13	0.129
Ga/HZSM-5 (IWI)	353	246	0.437	0.129	0.308
Ga/HZSM-5 (IE)	369	246	0.468	0.129	0.339
20CLD/Ga/HZSM-5	303	234	0.297	0.123	0.174
30CLD/Ga/HZSM-5	295	230	0.305	0.121	0.184
50CLD/Ga/HZSM-5	292	229	0.285	0.12	0.165
2C/30CLD/Ga/HZSM-5	268	216	0.235	0.113	0.122
3C/30CLD/Ga/HZSM-5	240	192	0.203	0.101	0.102
0.2PtGa/HZSM-5	363	246	0.442	0.129	0.313
0.2ZnGa/HZSM-5	320	218	0.408	0.118	0.29
0.2LaGa/HZSM-5	356	252	0.432	0.133	0.299
0.2PGa/HZSM-5	362	258	0.444	0.136	0.308
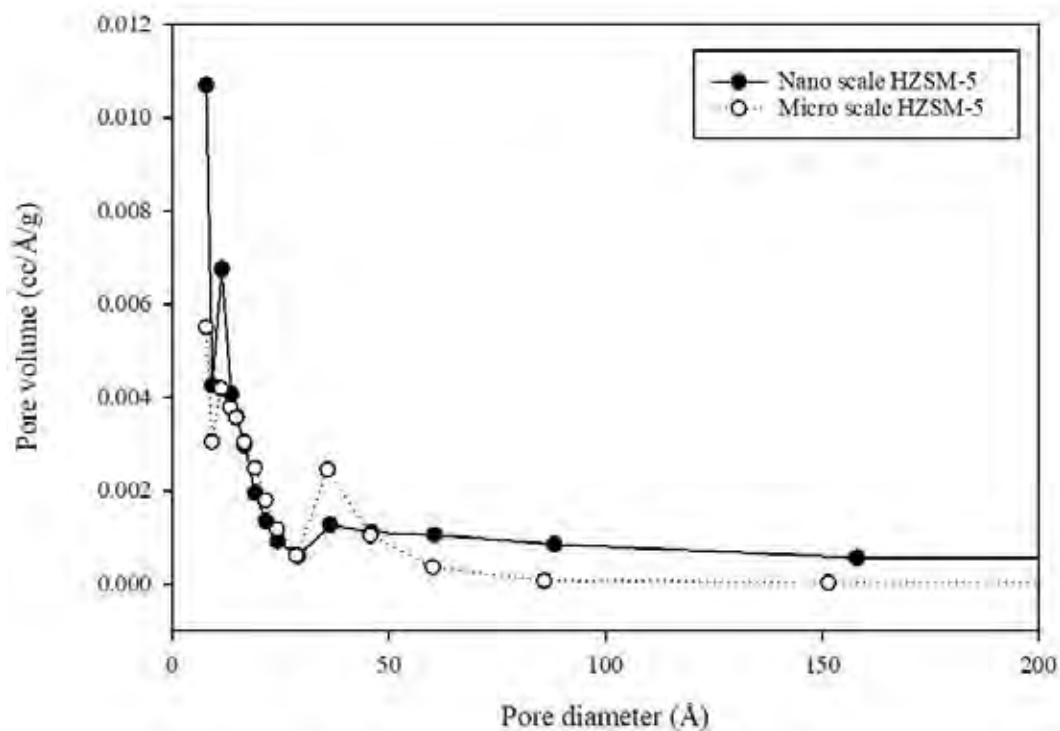
Figure 4.1 Pore size distribution of nano scale HZSM-5 and micro scale HZSM-5.

4.1.2 X-ray Diffraction

The MFI topology of parent micro scale, parent nano scale, and modified HZSM-5 catalyst were confirmed by XRD results. The scanning region of diffraction pattern was 5-50°, which showed the important diffraction peak of the HZSM-5 zeolite (ref). The X-ray diffraction pattern showed the remaining in the crystal structure of catalysts according to the method of gallium loading, silylation and co-impregnation with promoter, as can be seen in Figure 4.2. The XRD peak represented the HZSM-5 in MFI structure. The boarding of typical peak, especially 2θ = 24.3° in XRD pattern was observed in the parent nano scale HZSM-5 which probably described to their nanosized crystallinities compared to micro scale HZSM-5 (Liang *et al.*, 2016) and it was resulting from the easily dealumination or desilication during calcination because nanosized showed the high energy of Si and Al atom on surface leading to easily extract from framework (Zhang *et al.*, 2001). From Figure 4.2, there was no peak corresponding to Ga_2O_3 peak (2θ = 31.7 and 35.2°) on the modified

catalyst. This result could be indicated from the high dispersion of gallium in the modified catalysts. The silylated catalysts showed the decreasing in peak intensities of XRD pattern compared to the parent nano scale HZSM-5. This result came from the decreasing of surface areas which was probably caused from the deposition of TEOS molecules on the external surface of Ga/HZSM-5 (Kilic *et al.*, 2010). The co-impregnated catalyst with Pt, Zn, La and P to Ga/HZSM-5 remained the structure of HZSM-5 and there was no additional peak due to the good dispersion of promoter on the HZSM-5 surface (Ni *et al.*, 2011).
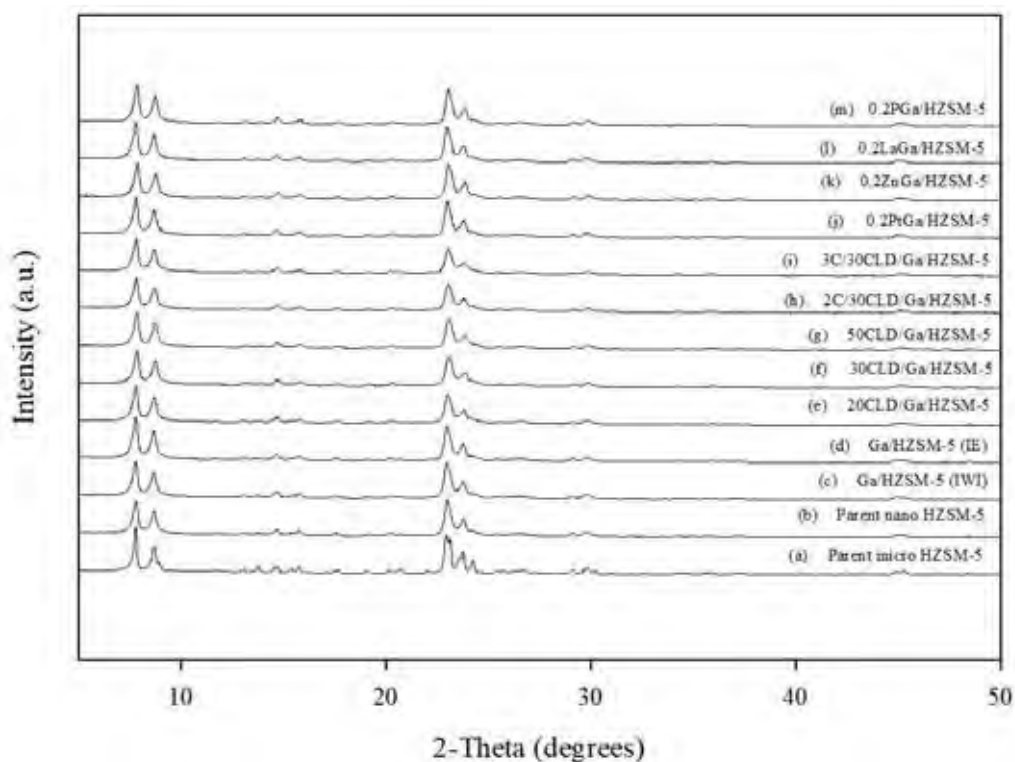
Figure 4.2 XRD patterns of (a) Parent micro HZSM-5, (b) Parent nano HZSM-5, (c) Ga/HZSM-5 (IWI), (d) Ga/HZSM-5 (IE), (e) 20CLD/Ga/HZSM-5, (f) 30CLD/Ga/HZSM-5, (g) 50CLD/Ga/HZSM-5, (h) 2C/30CLD/Ga/HZSM-5, (i) 3C/30CLD/Ga/HZSM-5, (j) 0.2PtGa/HZSM-5, (k) 0.2LaGa/HZSM-5, (l) 0.2ZnGa/HZSM-5, and (m) 0.2PGa/HZSM-5.

4.1.3 <u>Field Emission Scanning Electron Microscope (FE-SEM)</u>

The FE-SEM images of parent nano scale HZSM-5 and parent micro scale HZSM-5 are shown in Figure 4.3. which confirmed that the particle size of parent nano scale HZSM-5 was smaller than that of parent micro scale HZSM-5. Moreover, the decreasing particle size of HZSM-5 showed the increase of external surface areas which related to the BET results (Song *et al.*, 2004). Furthermore, SEM image of 3C/30CLD/Ga/HZSM-5 showed the layer of amorphous from the TEOS molecules on the external surface which passivated the external acid site and narrowed the pore mouth of HZSM-5 (Teng *et al.*, 2011).
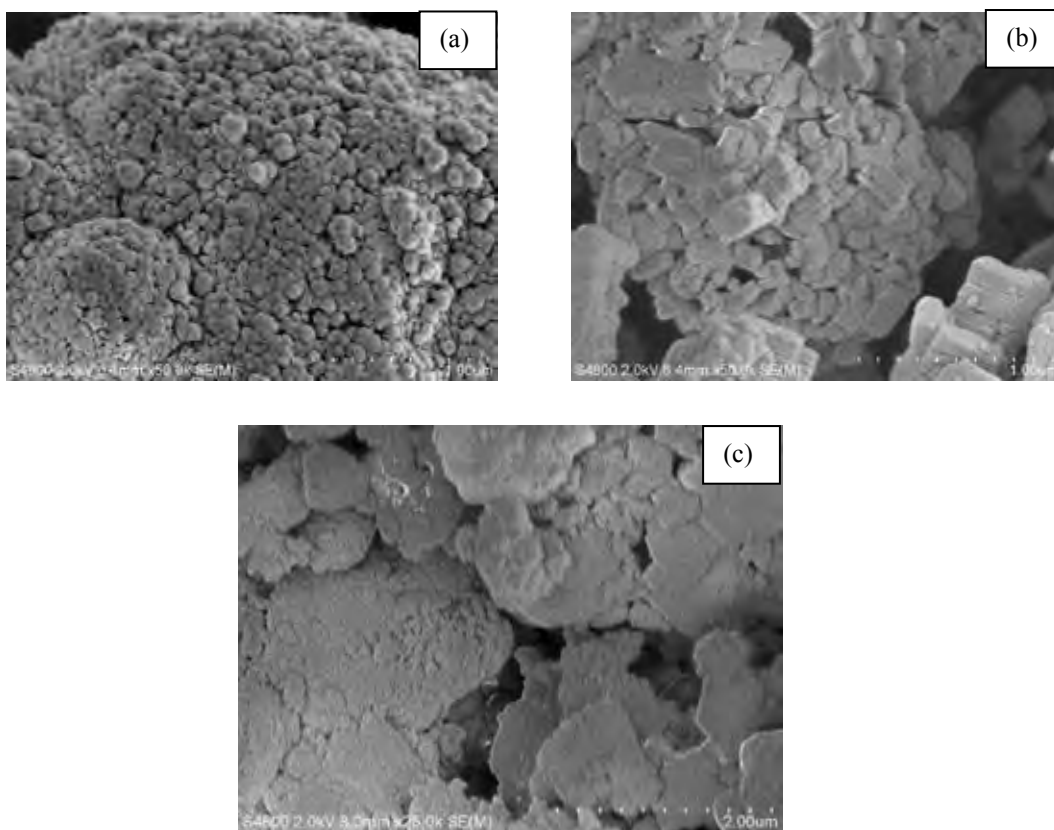
Figure 4.3 FE-SEM images of (a) parent nano HZSM-5, (b) parent micro HZSM-5 and (c) 3C/30CLD/HZSM-5.

4.1.4 ^{27}Al MAS NMR

MAS NMR of ^{27}Al of the modified HZSM-5 catalysts showed the signal at 0 ppm represented the octahedral aluminium or aluminium extra-framework and 55 ppm represented the tetrahedral aluminium or aluminium framework (Niwa *et al.,* 2012). From Figure 4.4, the results showed that co-impregnation with ammonium hydrogen phosphate exhibited higher intensity of signal at 55 ppm than Ga/HZSM-5 because NH$_4$$^+$ from precursor had different cation with Si-OH-Al groups which led to repair the wrecked Al-O-Si and increase amount of aluminium framework. Moreover, 0.2PGa/HZSM-5 showed the increasing in signal at 48 ppm and 28 ppm relating to dislodged tetrahedrally or pentahedrally coordinated aluminium framework due to the formation of two terminal Al-OH groups and compensation with one proton to negative charge to framework (van der Bij *et al.*, 2014).
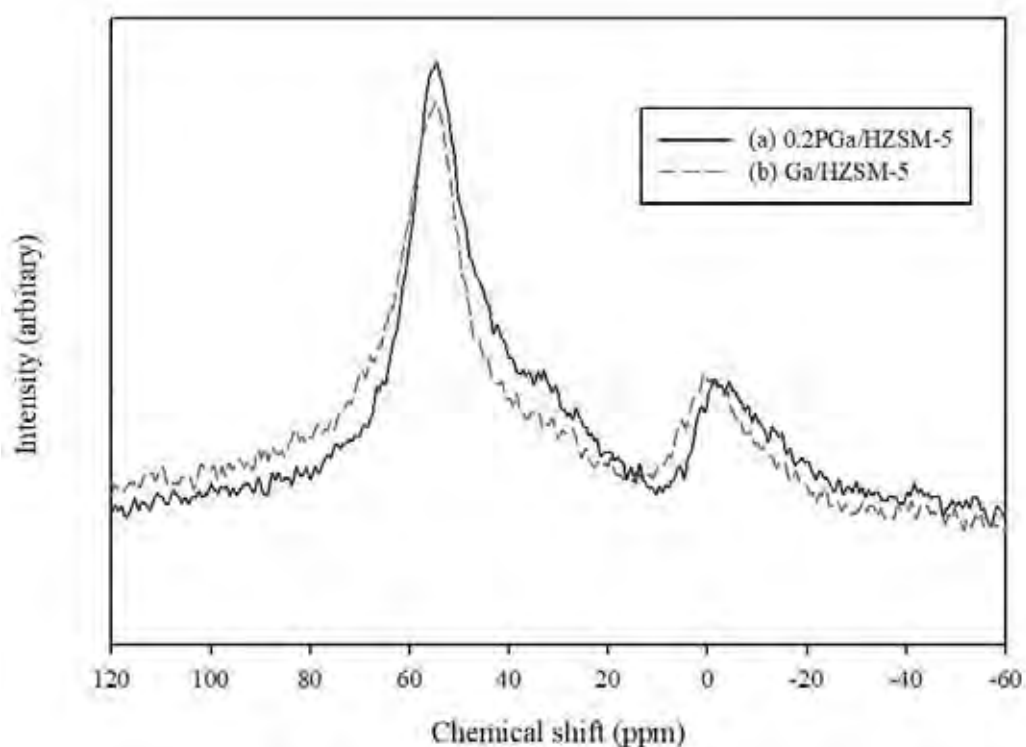
Figure 4.4 MAS NMR of ^{27}Al of (a) 0.2PGa/HZSM-5, (b) Ga/HZSM-5.

4.1.5 Temperature Programmed (H$_2$) Reduction TPR

Temperature programmed (H$_2$) reduction (TPR) profiles for the parent and various modified HZSM-5 catalysts are shown in Figure 4.5. The parent HZSM-5 and all of modified HZSM-5 showed the board peak around temperature 100 °C which related to characteristic peak of low Si/Al ratios of HZSM-5 (Todorova et $al.$, 2005). The incorporation of gallium to HZSM-5 zeolite present the two oxide phase. First, small Ga$_2$O$_3$ weakly interacts with zeolite at temperature of 550 °C. The ion-exchanged Ga/HZSM5 showed the small board peak at a temperature starting around 500 °C from the reduction of Ga$_2$O$_3$ in the micropore space to form Ga$_2$O due to the well-dispersed of gallium which interacted with the zeolite (Todorova et $al.$, 2004). Second, the higher temperature around 670 °C represented the strong interaction of dispersed gallyl ion (GaO)$^+$ species with HZSM-5. The impregnated Ga/HZSM-5 started this peak at lower temperature which lower interacted with zeolite than ion-exchanged catalyst and extended this peak over high temperature and did not appear complete at highest temperature. Southward and co-workers found that the reduction of Ga$_2$O$_3$ can be completed at temperature higher than 1,000 °C (Southward et $al.$, 1996). The ion-exchanged catalyst showed the large part board peak and shifted at high temperature due to the larger gallium oxide particle in the external surface of HZSM-5.
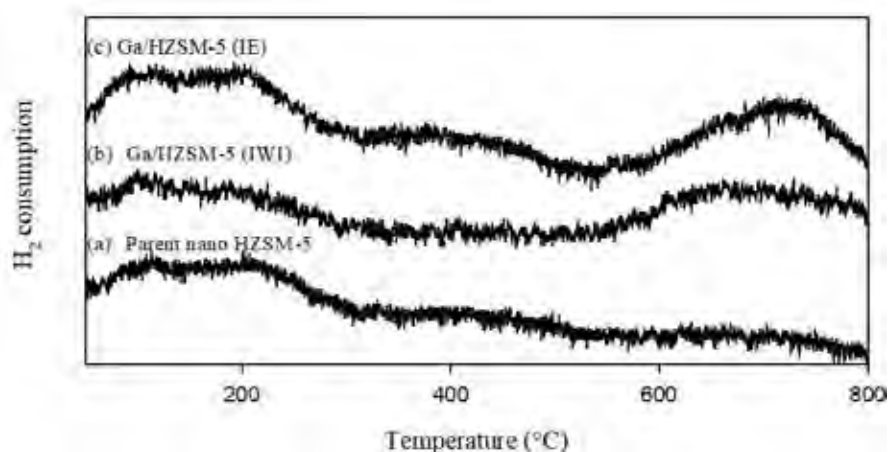
Figure 4.5 TPR profiles of (a) HZSM-5, (b) Ga/HZSM-5 (IWI), (c) Ga/HZSM-5 (IE).

4.1.6 Ammonia-TPD

Temperature programmed desorption of ammonia (NH₃-TPD) was applied to analyze the total acid strength and acidity of parent and modified Ga/HZSM-5 catalysts, as shown in Figure 4.6. The NH₃-TPD could be divided into three types of desorption peaks as list in Table 4.2. The quantities of weak, medium, and strong acid sites were measured by the amount of ammonia desorption at 100-200, 200-300, and 300-550 °C, respectively. The parent nano scale HZSM-5 exhibited the highest amount of acid site especially, the strong acid sites. After loading gallium to parent HZSM-5, the strong acid site decreased because gallium could reduce the number of surface acid sites. Moreover, the increasing in medium acid sites was a result from the incorporation of gallium species such as GaO^+, Ga^{3+}, or GaH_2^+ to zeolite framework (Choudhary *et al.*, 2000). After the silylation, the increasing TEOS concentration led to slightly decrease the total acidity, including with weak, medium and strong acid sites due to the low amount of inert silica layer deposition on the external acid sites, as shown in Table 4.2. However, the multicycle silylation significantly decreased the strong and medium acid site to generate more weak acid sites because the silica layer could form uniformly and reduce the access of molecule to internal acid site including the blockage of pore mouth (Weber *et al.*, 1998). Moreover, the multicycle silylaltion shift to lower temperature due to the decrease in weak acid strength. The co-impregnation with lanthanum and zinc showed obviously effect in decreasing of the strong acid sites and increasing in weak and medium acid sites due to the formation of hydroxy lanthanum cations species in ZSM-5 channels and exchanging between Zn^{2+} and $(AlO)^-$ with zeolite (Niu *et al.*, 2014). Furthermore, the addition with platinum to Ga/HZSM-5 could promote the more acidity, especially strong acid sites (Liu *et al.*, 2015). However, the phosphorous co-impregnated catalyst exhibited the decreasing total acidity and increasing medium acid sites which relating to the partial dealumination and the formation of local SAPO interfaces.

Figure 4.6 Ammonia-TPD (NH$_3$-TPD) profiles of (a) parent nano HZSM-5, (b) Ga/HZSM-5 (IWI), (c) Ga/HZSM-5 (IE), (d) 20CLD/Ga/HZSM-5, (e) 30CLD/Ga/HZSM-5, (f) 50CLD/Ga/HZSM-5, (g) 2C/30CLD/Ga/HZSM-5, (h) 3C/30Cld/Ga/HZSM-5, (i) 0.2PtGa/HZSM-5, (j) 0.2ZnGa/HZSM-5, (j) 0.2LaGa/HZSM-5, and (k) 0.2PGa/HZSM-5. The mass monitored was ammonia (m/e=17).

Table 4.2 The total acidity, detected by NH$_3$-TPD of the parent nanoscale HZSM-5 and modified Ga/HZSM-5

Catalyst	Total Acidity (µmol/g)			
	Weak	Medium	Strong	Total
parent nano HZSM-5	140	594	1,348	2,082
Ga/HZSM-5 (IWI)	225	552	688	1,465
Ga/HZSM-5 (IE)	178	558	658	1,394
20CLD/Ga/HZSM-5	405	626	325	1,355
30CLD/Ga/HZSM-5	368	569	295	1,232
50CLD/Ga/HZSM-5	331	512	266	1,109
2C/30CLD/Ga/HZSM-5	288	374	138	800
3C/30CLD/Ga/HZSM-5	238	268	76	582
0.2PtGa/HZSM-5	138	512	918	1,568
0.2ZnGa/HZSM-5	152	448	546	1,146
0.2LaGa/HZSM-5	193	457	512	1,162
0.2PGa/HZSM-5	180	506	569	1,256

4.1.7 <u>Isopropylamine-TPD</u>

Temperature programmed desorption of isopropylamine (IPA-TPD) was performed to analyze the Brønsted acid sites of modified HZSM-5 as shown in Figure 4.7. The results showed that the Brønsted acid sites of Ga/HZSM-5 which detected at temperature 350 °C significantly decreased due to the exchange of partially acidic proton with the gallium species compared to parent HZSM-5 (Xiao *et al.*, 2015). Moreover, the silylation with TEOS to Ga/HZSM-5 showed the decrease in Brønsted acid sites from the deposition of inert silica layer and elimination external acid sites of Ga/HZSM-5. The multicycle silylation to Ga/HZSM-5 exhibited the significant decreasing in Brønsted acid sites more than the effect of TEOS concentration because

multicycle silylation formed the uniformity of inert silica layer, implying the success in deposition of inert silica layer to external acid site of HZSM-5.

Table 4.3 The total Brønsted acidity, detected by IPA-TPD of parent HZSM-5 and the modified Ga/HZSM-5 zeolites

Catalyst	Brønsted Acidity (µmol/g)
parent nano HZSM-5	1,227
Ga/HZSM-5 (IWI)	927
Ga/HZSM-5 (IE)	1,141
20CLD/Ga/HZSM-5	906
30CLD/Ga/HZSM-5	910
50CLD/Ga/HZSM-5	805
2C/30CLD/Ga/HZSM-5	693
3C/30CLD/Ga/HZSM-5	328
0.2PtGa/HZSM-5	1,107
0.2ZnGa/HZSM-5	899
0.2LaGa/HZSM-5	802
0.2PGa/HZSM-5	960

The measurement amount of Brønsted acid sites was performed by desorption of propylene, as can be seen in Table 4.3. 0.2PtGa/HZSM-5 showed the increase Brønsted acid sites at higher temperature compared to Ga/HZSM-5 because platinum could promote the strong acid sites relating to Brønsted acid sites. The co-impregnation with lanthanum and zinc to Ga/HZSM-5 slightly decreased the Brønsted acid sites because it could be converted into the Lewis acid sites (Li *et al.*, 2014). Moreover, the addition with phosphorous exhibited the slightly increased the Brønsted acid sites due to the recovering some Si-OH-Al groups, relating to the result from ^{27}Al MAS NMR, as show in Figure 4.4.

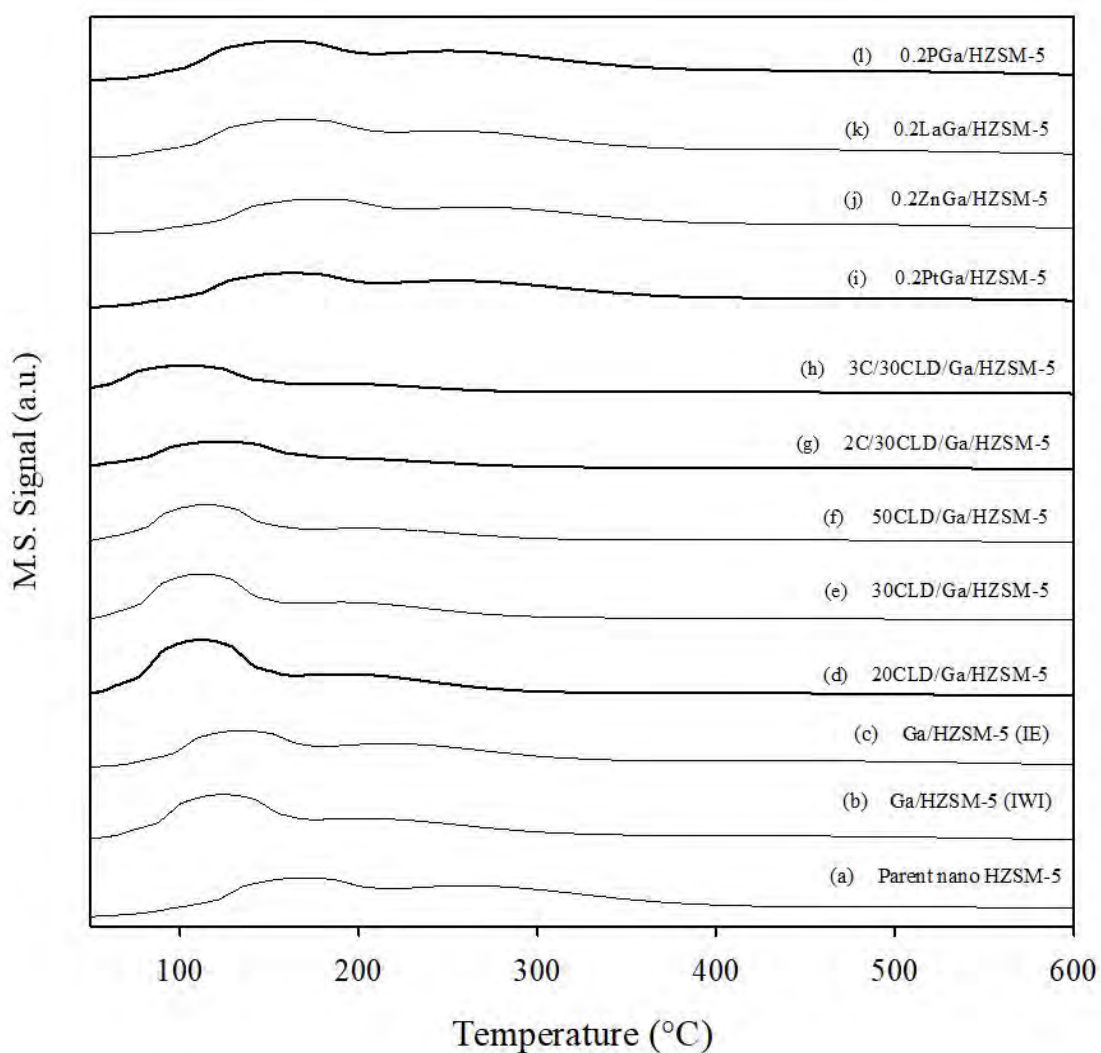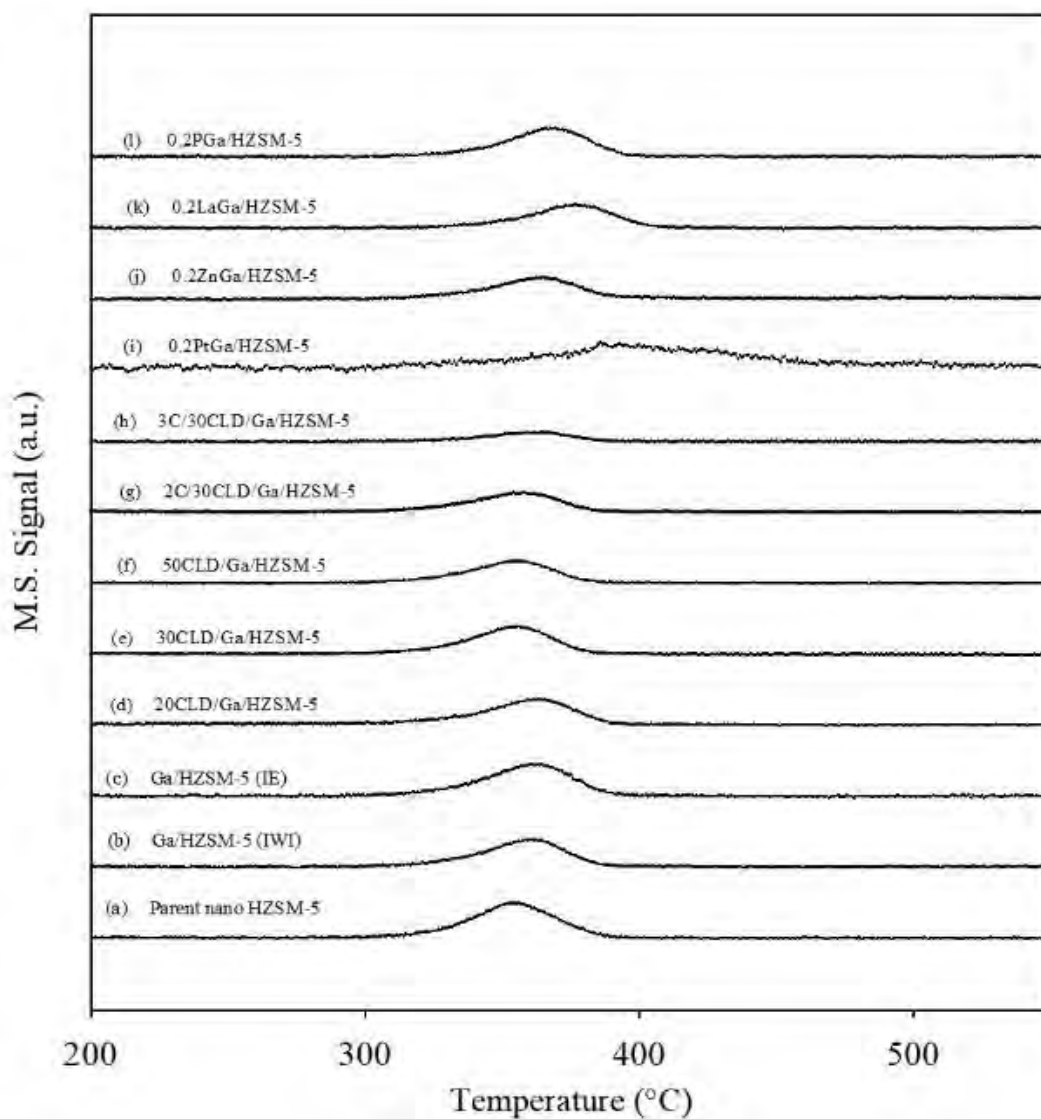**Figure 4.7** Isopropylamine-TPD (IPA-TPD) profiles of (a) parent nano HZSM-5, (b) Ga/HZSM-5 (IWI), (c) Ga/HZSM-5 (IE), (d) 20CLD/Ga/HZSM-5, (e) 30CLD/Ga/HZSM-5, (f) 50CLD/Ga/HZSM-5, (g) 2C/30CLD/Ga/HZSM-5, (h) 3C/30Cld/Ga/HZSM-5, (i) 0.2PtGa/HZSM-5, (j) 0.2ZnGa/HZSM-5, (j) 0.2LaGa/HZSM-5, and (k) 0.2PGa/HZSM-5. The mass monitored was propylene (m/e=41).

4.1.8 Temperature Programmed (O$_2$) Oxidation (TPO)

Temperature programmed (O$_2$) oxidation (TPO) profiles of the spent parent HZSM-5 and modified HZSM-5 catalysts are shown in Figure 4.8. The results indicated that the parent nano scale HZSM-5 exhibited the lower coke formation compared with parent micro scale HZSM-5. The presence in the mesopore and macropore in the smaller size catalyst, confirmed by BET analysis in Table 4.1, it could reduce the diffusional limitations in the channel of catalysts (Lucas *et al.*, 1997). After incorporation gallium to parent nano HZSM-5, the higher coke deposition were formed at the lower temperature due to the decrease in strong acid site and increase in weak acid sites (Kwak *et al.*, 1994).
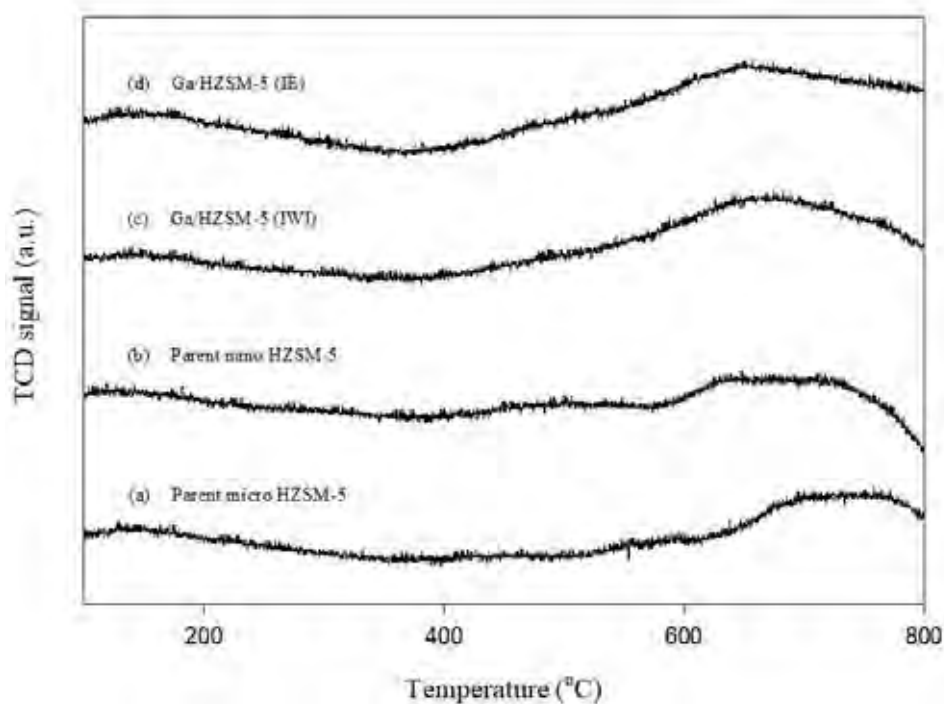
Figure 4.8 Temperature programmed (O$_2$) oxidation (TPO) profiles of spent catalysts (a) Parent micro HZSM-5, (b) Parent nano HZSM-5, (c) Ga/HZSM-5 (IWI), and (d) Ga/HZSM-5 (IE).

The TPO profiles of modified Ga/HZSM-5 catalysts are shown in Figure 4.9 exhibited the lower amount of coke formation slightly compared to unsilylated catalysts because the deposition of inert silica layer could eliminate the external acid sites. Especially, the multicycle silylation showed the coke formation at lower temperature because of the increasing in the effect of passivation of external acid sites. The addition of phosphorous and lanthanum showed the higher carbon deposition at lower temperature. due to generation the new Brønsted acid which slightly formed the carbon deposition and promoted the catalytic performance (Zhao et al., 2007). The co-impregnation of Pt to Ga/HZSM-5 exhibited the coke formation at high temperature which higher than 800 °C and showed the lower amount of hydrocarbon deposition because platinum had the role in the hydrogen spillover and hydrogenation to catalyst which improved the stability of catalyst (Todorova et al., 2004).
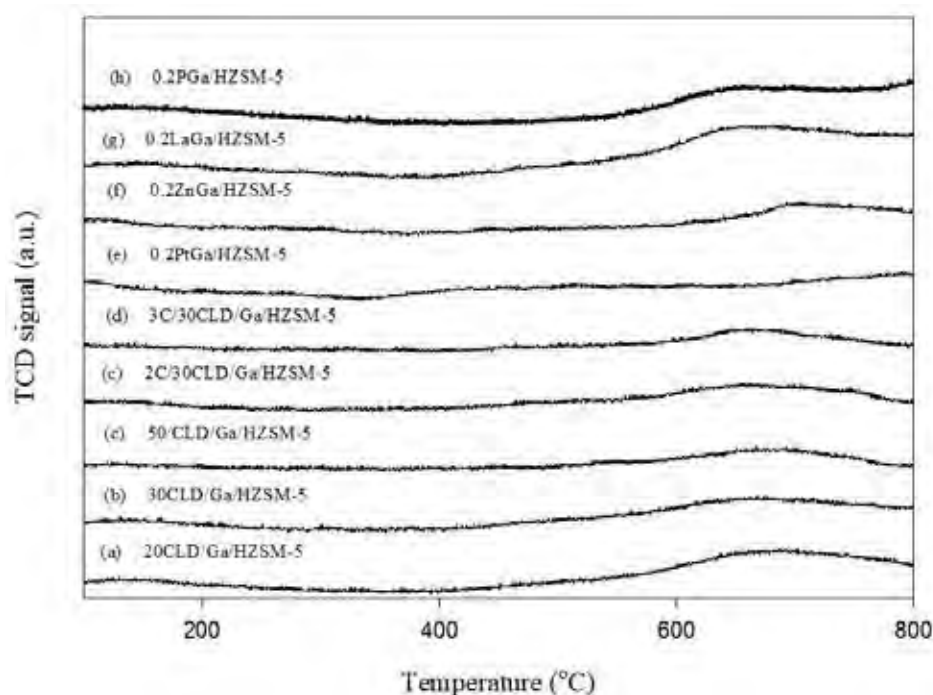
Figure 4.9 Temperature programmed (O_2) oxidation (TPO) profiles of spent
(a) 20CLD/Ga/HZSM-5, (b) 30CLD/Ga/HZSM-5, (c) 50CLD/Ga/HZSM-5,
(d) 2C/30CLD/Ga/HZSM-5, (e) 3C/30CLD/Ga/HZSM-5, (f) 0.2PtGa/HZSM-5,
(g) 0.2LaGa/HZSM-5, (h) 0.2ZnGa/HZSM-5, and (i) 0.2PGa/HZSM-5.

4.2 Catalytic Activity Testing

The catalytic activity testing was conducted with parent HZSM-5 and modified catalysts on their catalytic activity and selectivity in n-pentane converting into aromatics. The author classified the obtained products into three main groups; (1) light paraffins: propane, methane, ethane, and butane, (2) light olefins: propylene, acetylene, ethylene, 1-butene, and iso-butene, (3) aromatics: benzene, toluene, ethylbenzene, and mixed-xylene (p-xylene, m-xylene, and o-xylene).

4.2.1 Effect of Crystal Size of Parent Zeolite

In this study, the effect of crystal sizes of parent HZSM-5 which are micro scale and nano scale is introduced in n-pentane aromatization. According to Table 4.4, the nano size of parant HZSM-5 exhibited higher aromatic selectivity in n-pentane aromatization reaction. Though the main reaction occurs over micropore, the higher aromatics selectivity over the parent nano scale HZSM-5 could be obtained from the presence of mesopores and macropores volume in smaller crystal size which enhance molecular diffusion of aromatics. Moreover, the higher of light olefins selectivity could also obtain from the nano size HZSM-5 zeolite because the diffusion limitation was reduced with the decreasing particle size (Rownaghi *et al.*, 2012). However, the selectivity of p-xylene over mixed xylenes in both catalysts show the close value to the thermodynamic equilibrium which is around 23%. It is the result from the isomerization of p-xylene to other isomers.

Table 4.4 Products selectivity and conversion of *n*-pentane over parent nano size and micro size HZSM-5 catalysts (Reaction condition: 500 °C, 1 atm, WHSV = 5 h^{-1}, and TOS = 130 min)

Conversion and products selectivity (%)	Catalyst	
	Parent Nano HZSM-5	Parent Micro HZSM-5
Conversion (%)	78.52	86.26
Products Selectivity (%)		
Light paraffins	63.75	70.61
Light olefins	23.31	17.87
Aromatics	12.94	11.52
Benzene	2.25	3.62
Toluene	6.12	5.56
Mixed xylenes	4.57	2.38
p-xylene in xylenes	23.10	23.80

4.2.2 The Effect of Gallium Loading Method

The effect of Ga loading to parent nano scale HZSM-5 on catalytic activity in *n*-pentane aromatization was investigated. The results are illustrated in Figure 4.10, the incorporation with gallium both incipient wetness impregnation and ion-exchange method significantly improved the aromatics selectivity. In addition, the lower selectivity of light paraffins and olefins in these catalysts because gallium could improve the dehydrogenation in aromatization reaction (Nash *et al.*, 1996). Gallium promoted the dehydrogenation of light paraffins to olefin which is the important intermediate to produce aromatics compound.
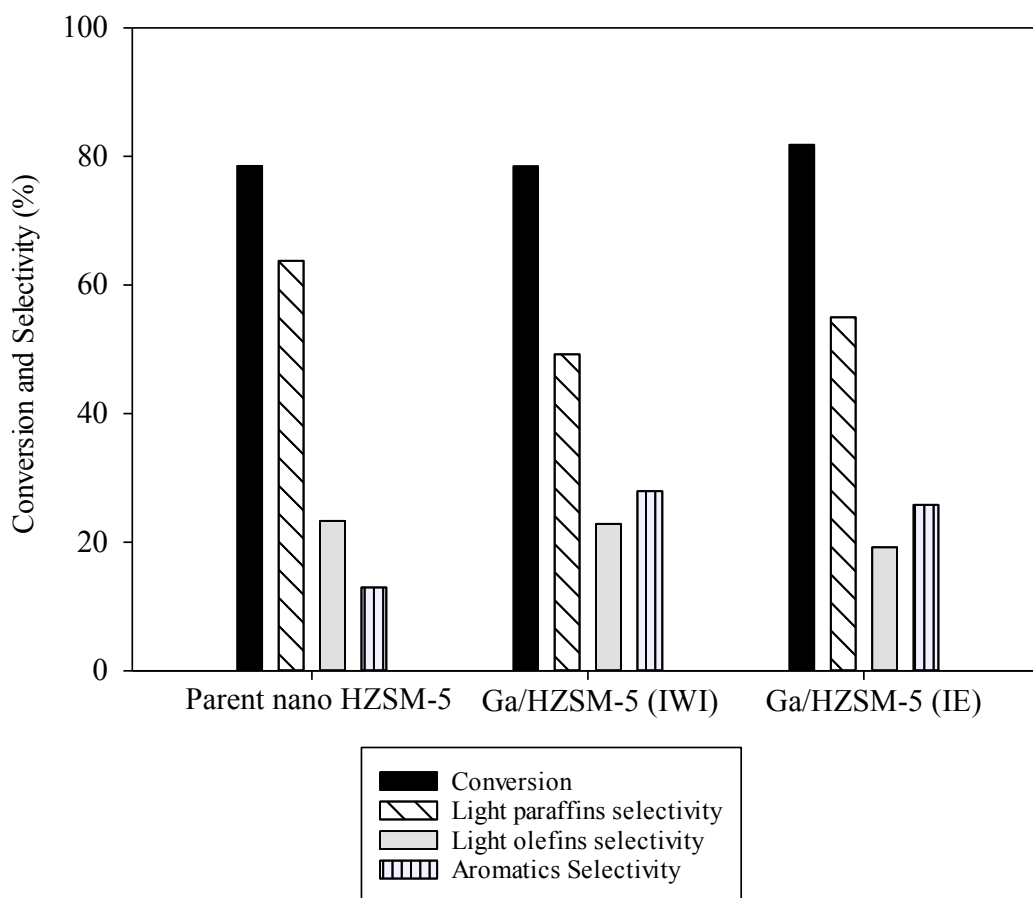
Figure 4.10 Effect of method of gallium loading to nano size HZSM-5 zeolite on the *n*-pentane conversion and products distribution (Reaction condition: 500 °C, 1 atm, WHSV = 5 h^{-1} and TOS = 130 min).

Aromatics selectivity of *n*-pentane aromatization in both incipient wetness impregnation and ion-exchange method are shown in the Figure 4.11 The result showed that the impregnated Ga/HZSM-5 exhibited the higher aromatic selectivity than the ion-exchanged Ga/HZSM-5. The impregnated Ga/HZSM-5 presented the mobile gallium oxide and substituted the Brønsted acid sites by Ga$^+$ and GaH^{2+} which promoted the aromatics selectivity. The ion exchanged Ga/HZSM-5 showed the difficulty in reduction of gallium oxide phase and had more Brønsted acid sites as confirmed by Figure 4.5. For this reason, the ion-exchanged Ga/HZSM-5 slightly increased the conversion in *n*-pentane aromatization (Rane *et al.*, 2008).
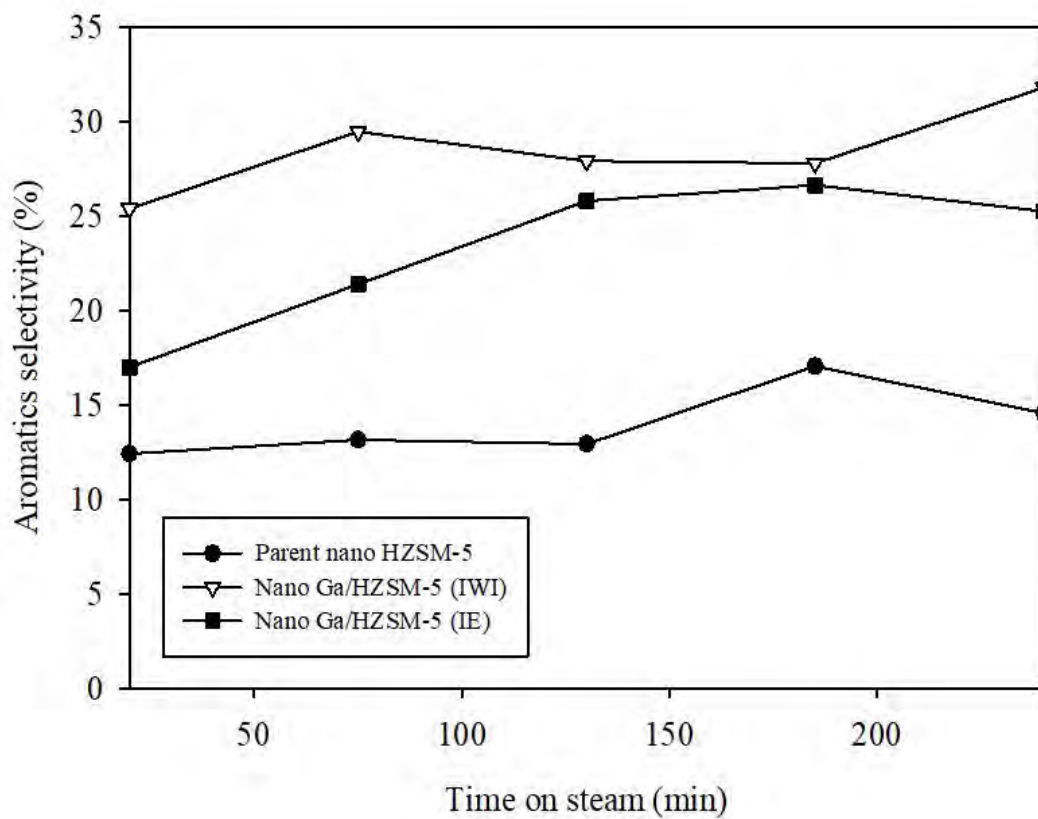
Figure 4.11 Effect of gallium loading method to nano size HZSM-5 zeolite on the *n*-pentane conversion to aromatics selectivity (Reaction condition: 500 °C, 1 atm, WHSV = 5 h^{-1} and TOS = 130 min).

4.2.3 Effect of TEOS Concentration in Silylation

The silylation with chemical liquid deposition (CLD) by loading TEOS had a significant effect on product selectivity especially the improvement of *p*-xylene in mixed xylene through the deposition of inert silica layer over external surface of zeolite (Teng *et al.*, 2011). This study showed that the removal of external acid sites and also had the formation of inert silica layer in pore-narrowing that could decrease the catalytic activity in alkylbenzene disproportionation (Bauer *et al.*, 2004). In this study, tetraethyl orthosilicate (TEOS) with kinetic diameter around 1.03 nm was introduced to Ga/HZSM-5 to deactivate the external acid sites of nano scale zeolites. The deposition of 20 %vol TEOS resulted in the decrease activity in *n*-pentane aromatization but slightly improved of *p*-xylene selectivity in mixed xylene also

slightly increased from 21% to 30% due to the passivation of some external acid sites over Ga/HZSM-5. The chemical liquid deposition of TEOS for smaller crystal size had the lower effect which compared to larger crystal size (Zheng *et al.*, 2003). The catalytic conversion over 20CLD/Ga/HZSM-5, 30CLD/Ga/HZSM-5, and 50CLD/Ga/HZSM-5 was lower than Ga/HZSM-5 resulting from the decreasing in surface areas and the passivation some external surface areas of HZSM-5, as shown in Figure 4.12.

Figure 4.12 Effect of TEOS loading in silylatiion Ga/HZSM-5 on *n*-pentane conversion. (Reaction condition: 500 °C, 1 atm, and WHSV = 5 h^{-1}).

The *p*-xylene selectivity could be enhanced due to the formation of inert silica layer on external surface of HZSM-5 zeolite. Figure 4.13 shows the effect of the amount of TEOS in the chemical liquid deposition on Ga/HZSM-5. It could be seen that the increasing of TEOS loading on Ga/HZSM-5 could promote the *p*-xylene selectivity in mixed xylenes. The deposition with 30% vol TEOS on Ga/HZSM-5 improved the *p*-xylene selectivity up to 35% over mixed xylenes. However, when increasing the amount of TEOS to 50% vol showed the lower *p*-xylene selectivity in mixed xylenes than 30% vol because too much TEOS could cause the formation of an uneven inert silica layer and lowering shape selectivity (Teng *et al.*, 2011).

Figure 4.13 Effect of TEOS loading in silylation to Ga/HZSM-5 on the *n*-pentane conversion, products distribution, and *p*-xylene selectivity (Reaction condition: 500 °C, 1 atm, WHSV = 5 h^{-1} and TOS = 130 min).

4.2.4 Effect of CLD Multicycle

The multicycle of chemical liquid deposition was the one way to increase the amount of inert silica layer deposited on external surface of HZSM-5 zeolite and also improve the uniformity of inert silica layer (Zheng *et al.*, 2003). To study the effect of number of CLD cycle, the catalysts were prepared by suitable condition silylation with 30% vol TEOS in cyclohexane. The effect of number of cycle deposition with 30% vol TEOS in Ga/HZSM-5 on *n*-pentane conversion is shown in Figure 4.14. The result showed that increasing the number of silylation significantly decreased the surface areas with pore volume, and low acidities at external surface areas as compared to Ga/HZSM-5. In addition, this result led to decrease the conversion of *n*-pentane.
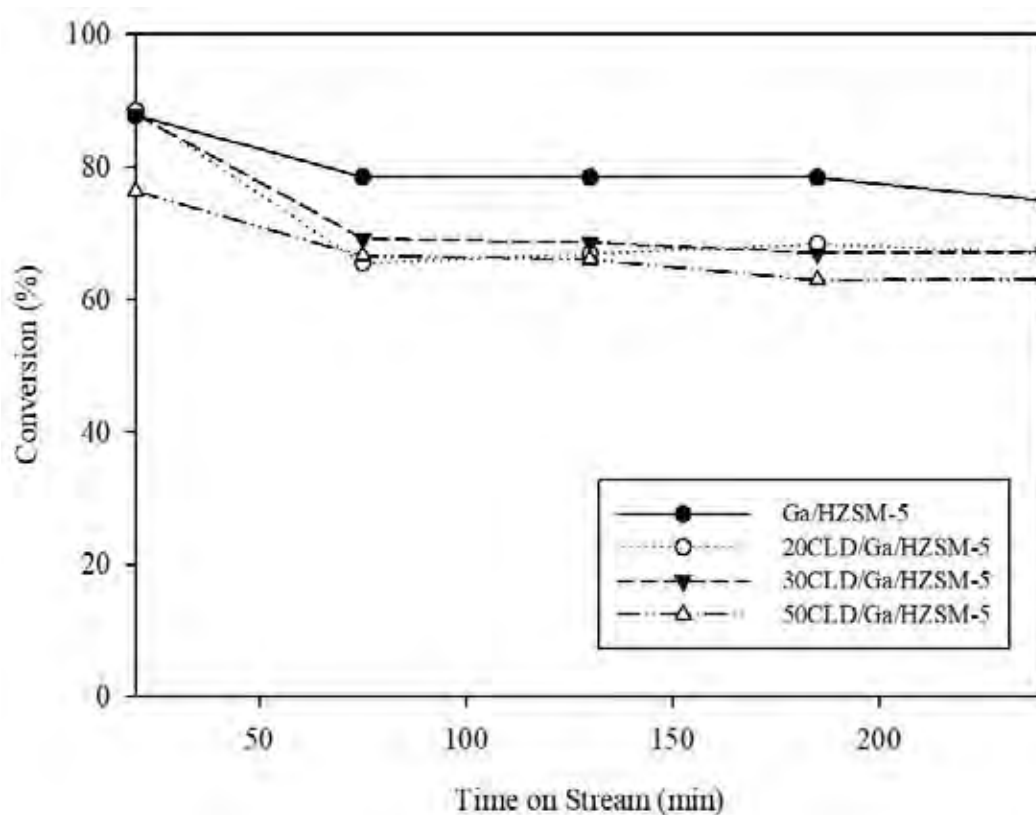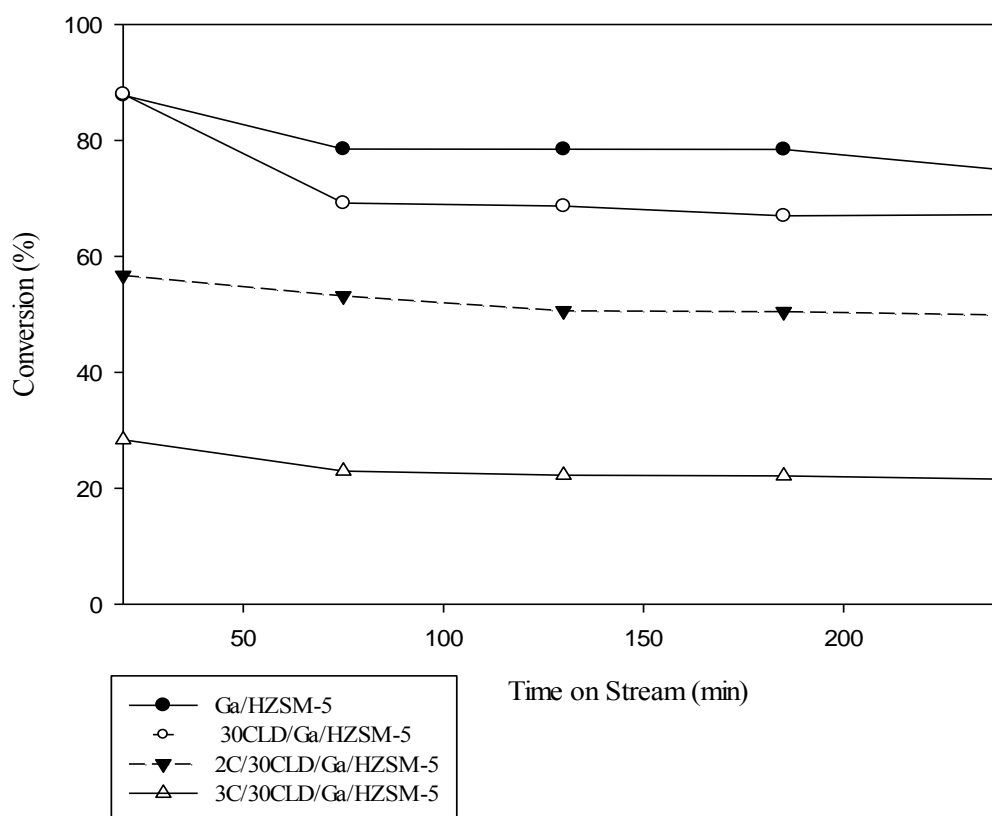

Figure 4.14 Effect of multicycle silylation to Ga/HZSM-5 on *n*-pentane conversion. (Reaction condition: 500 °C, 1 atm, and WHSV = 5 h^{-1}).

It could be seen that the multicycle silylation significantly improved the *p*-xylene selectivity in mixed xylenes due to the high effective to eliminate the external acid sites of nano scale HZSM-5 zeolite. The structure of HZSM-5 with 10 membered-ring channels was more favorable to the diffusion of *p*-xylene than o- and m-xylene but external acid site of zeolite affected to quick isomerization. The two cycle CLD treatment (2C/30CLD/Ga/HZSM-5) improved the *p*-xylene selectivity in mixed xylenes from 35% to 69% compared to one cycle CLD (30CLD/Ga/HZSM-5). Moreover, the improvement of *p*-xylene selectivity in mixed xylenes completely reached to 100% over the three cycle CLD (3C/The two cycle CLD treatment (2C/30CLD/Ga/HZSM-5) improved the *p*-xylene selectivity in mixed xylenes from 35% to 69% compared to one cycle CLD (30CLD/Ga/HZSM-5). Moreover, the improvement of *p*-xylene selectivity in mixed xylenes completely reached to 100% over the three cycle CLD30CLD/Ga/HZSM-5), as can be seen in Figure 4.15. The results also show that *m*- and *o*-xylene selectivity decreased with number of cycle CLD because multicycle silylation increased the uniformity of silica layer on external surface of nano scale HZSM-5 and these passivation of external acid sites could reduce the isomerization of *p*-xylene to *m*- and *o*-xylene. The surface area of nano scale HZSM-5 was spherical particle which led to increase the fraction of acid sites on external surface and in the pore mouth region compare to the micro scale HZSM-5. Furthermore, the small size of HZSM-5 zeolite presented the large amount of extra-framework aluminium which could narrow the pore of this particle. The multicycle silylation was necessary to narrow the pore mouth and deactivate the external acid sites. During the first cycle of silylation, TEOS reacted with acid sites located on the surface of zeolite and it could block other TEOS molecules to access the neighbouring acid sites for high concentration of acid sites particle. In the second and third cycle of silylation, the accessible acid sites were significantly decreased and increased the narrowing of the pore mouth with more TEOS molecules in the previous cycle which could penetrate the pore mouth of nano scale HZSM-5.

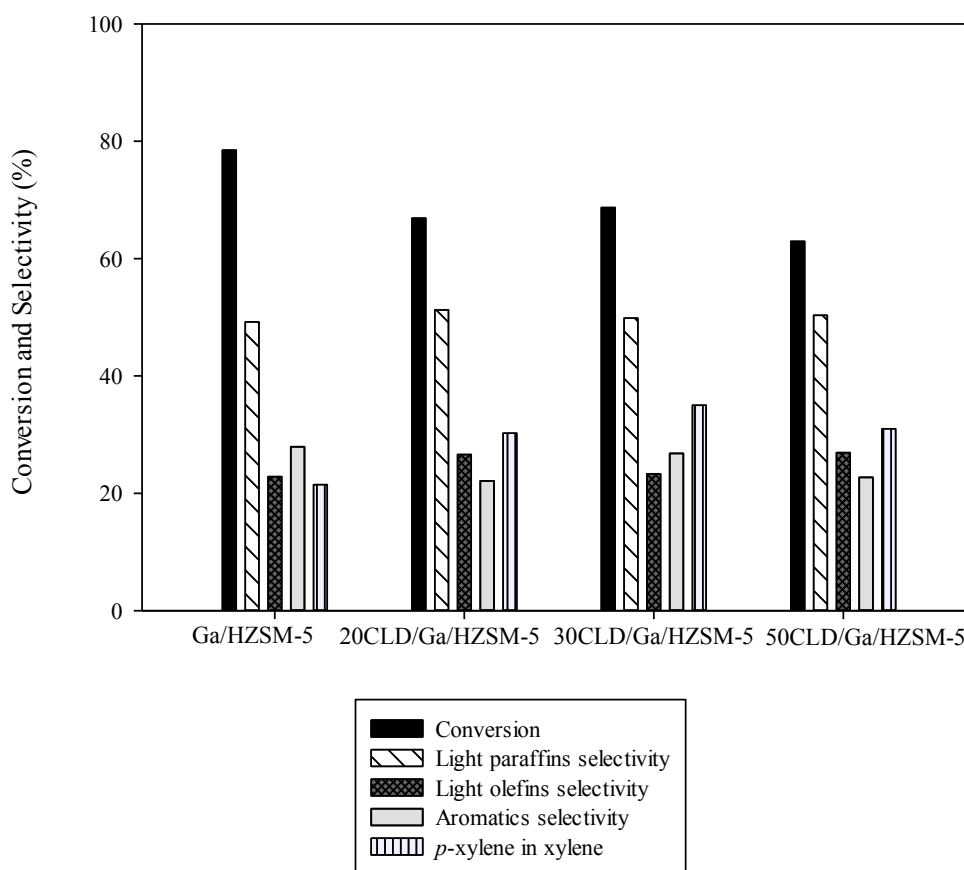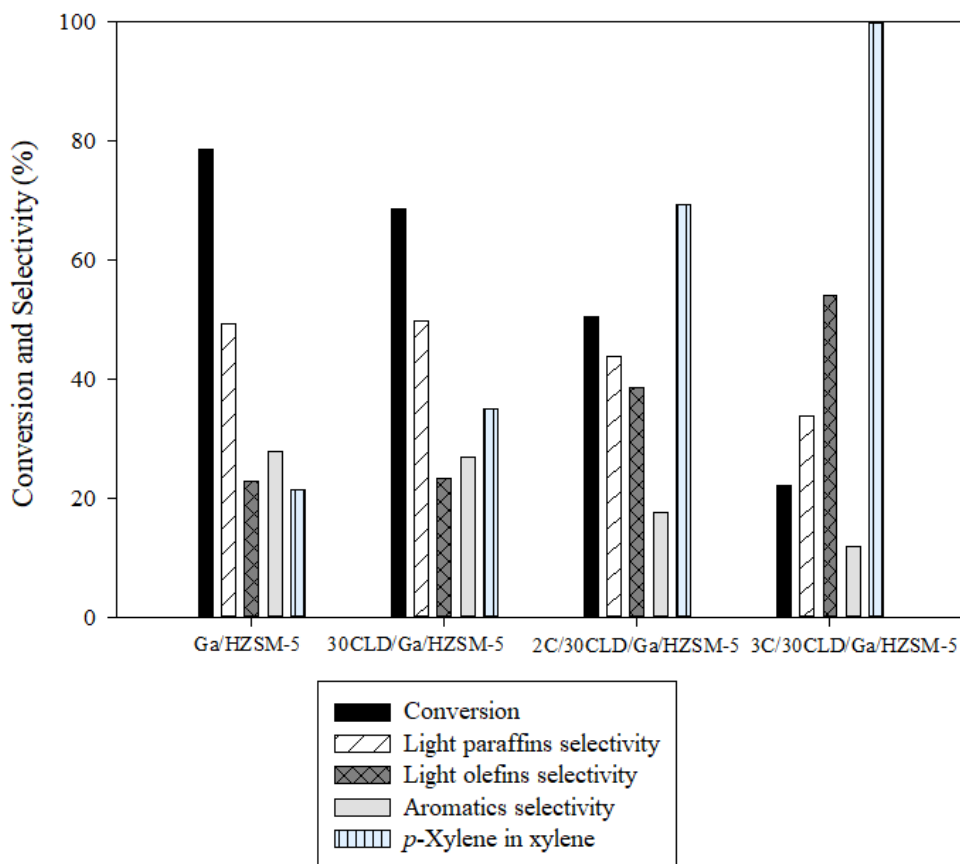**Figure 4.15** Effect of multicycle silylation to Ga/HZSM-5 on the *n*-pentane conversion, products distribution, and *p*-xylene selectivity (Reaction condition: 500 °C, 1 atm, WHSV = 5 h^{-1} and TOS = 130 min).

4.2.5 Effect of The Promoters

To study in the effect of promoter to enhance the stability and activity in *n*-pentane aromatization, introduction with 0.2%wt of Pt, Zn, La, and P as promoter to Ga/HZSM-5 was incorporated by co-impregnation method. The conversion of *n*-pentane is shown in Figure 4.16. The results indicated that the addition with Pt to Ga/HZSM-5 significantly improved the *n*-pentane conversion due to the increase in strong acid sites which related to TPD-NH$_3$ results. Moreover, the stability of 0.2PtGa/HZSM-5 was higher compared to other catalysts at same TOS because of the prevention in coke decomposition resulting from the decrease in weak acid sites

(Rasouli *et al.*, 2017). The co-impregnated catalyst with lanthanum of 0.2LaGa/HZSM-5 led to slightly increase stability of catalytic performance compared to Ga/HZSM-5 because lanthanum could reduce the coke decomposition on surface of catalyst (Ni *et al.*, 2011). The addition with small of zinc and phosphorous to Ga/HZSM-5 (0.2ZnGa/HZSM-5 and 0.2PGa/HZSM-5) showed the lower conversion compared to unpromoted catalyst, 0.2ZnGa/HZSM-5 could get the effect from the volatilization at high temperature and the formation of ZnO on external surface which slightly decreased the *n*-pentane conversion (Tshabalala *et al.*, 2015). Moreover, the strong acid sites would be remove after loading small amount of phosphorus due to formation of neutral SAPO interfaces which led to slightly decreased *n*-pentane conversion (Liu *et al.*, 2009).
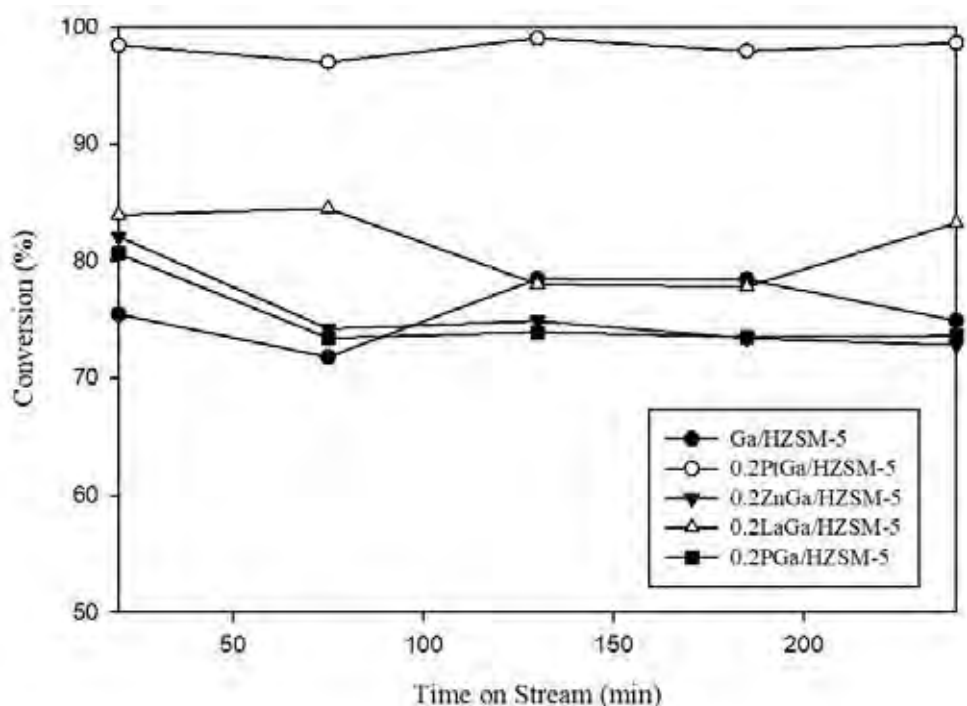
Figure 4.16 Effect of co-impregnation with promoter to Ga/HZSM-5 on on *n*-pentane conversion. (Reaction condition: 500 °C, 1 atm, and WHSV = 5 h^{-1}).

On the role of promoter to Ga/HZSM-5 in the improvement of aromatic selectivity was significantly observed in 0.2PGa/HZSM-5, as can be seen in Figure

4.17. The results indicated that the co-impregnation with phosphorous could increase the aromatic selectivity more than 10% compared to Ga/HZSM-5 resulting from the decreasing in the strong acid sites and generating more medium acidity. The increasing in medium acid sites came from the formation of dislodged tetrahedral aluminium framework species (van der Bij *et al.*, 2014). The combination between gallium and zinc showed the negative effect in aromatics selectivity due to the volatilization at high temperature (Zhou *et al.*, 2014). However, the addition with platinum in co-impregnated catalyst significantly decreased the aromatics selectivity because platinum exhibited the hydrogenolysis effect and promoted the strong acid sites which increased the undesirable products or light paraffins from side reaction (Shao *et al.*, 2017).

Figure 4.17 Effect of co-impregnation with promoter to Ga/HZSM-5 on the *n*-pentane conversion to aromatics selectivity. (Reaction condition: 500 °C, 1 atm, and WHSV = 5 h^{-1}).

The conversion and products distribution over Ga/HZSM-5 and promoted Ga/HZSM-5 are shown in Figure 4.18, the small amount of platinum to Ga/HZSM-5 significantly increased the *n*-pentane conversion due to generating strong acid sites, it also promoted the smaller alkanes because platinum had the effect in hydrogenation and hydrogenolysis. Firstly, *n*-pentane reacted with the strong acid sites in HZSM-5 which protonated the C-C bonds, generating smaller paraffins together with carbenium ions. Next, this carbenium ions could generate light olefins by B-scission but the light olefins formed into the small paraffins due to the hydrogenation effect of platinum species. In this result, the addition with small amount of platinum not only affected in the breaking of C-H bonds but it also formed new C-H bonds from the hydrogenolysis and hydrogenation which promoted the formation of smaller saturated hydrocarbon especially ethane and propane (Engelen *et al.*, 1985). For these reasons, after addition the small amount of strongly decreased the aromatics selectivity. Moreover, 0.2PGa/HZSM-5 showed the highest aromatic selectivity because phosphorous would react with zeolite to form the local SAPO interfaces and led to generate the new nest aluminium framework species such as extra framework aluminium species and P-OH group during thermal treatment, as confirmed by MAS NMR of ^{27}Al in Figure 4.4 (van der Bij *et al.*, 2015). Therefore. it slightly increased Brønsted acid sites and promoted the medium acid sites which had effect to convert the light paraffins and light olefins to aromatics compounds.
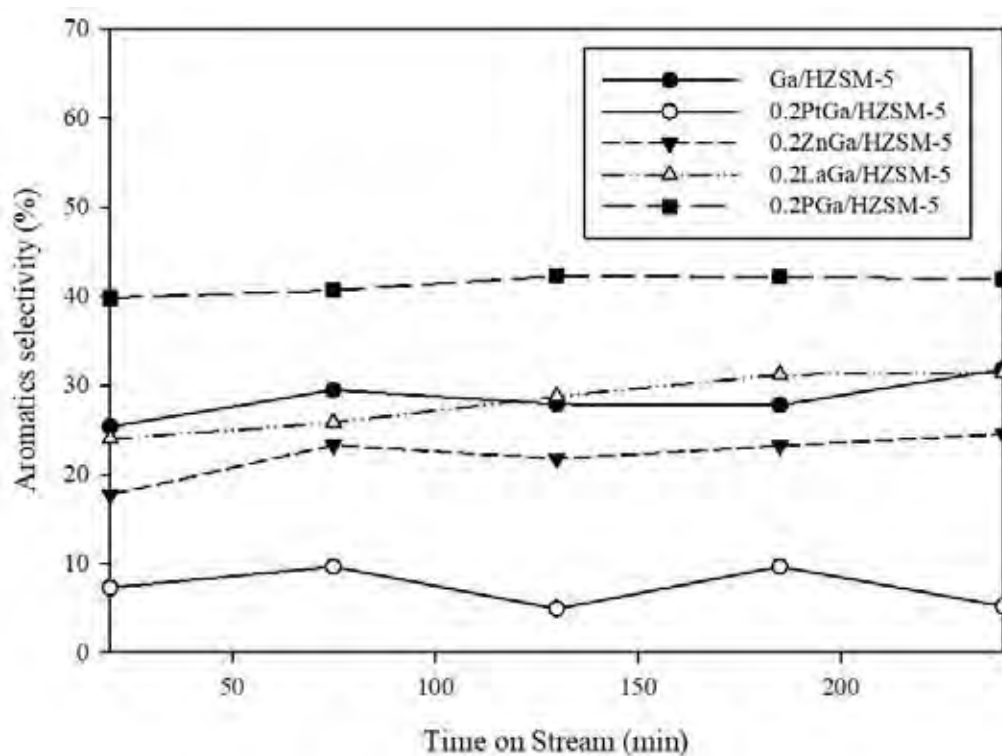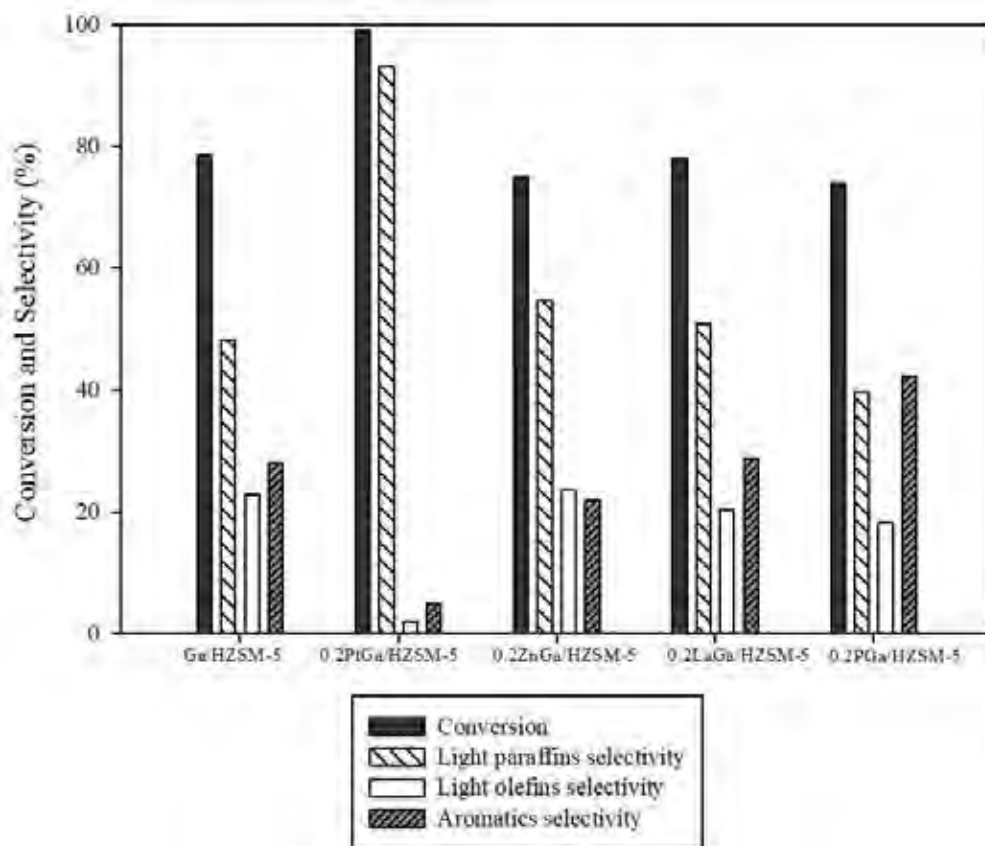
Figure 4.18 Effect of co-impregnation with promoter to Ga/HZSM-5 on the *n*-pentane conversion and products distribution (Reaction condition: 500 °C, 1 atm, WHSV = 5 h^{-1} and TOS = 130 min).

CHAPTER V
CONCLUSIONS AND RECOMMENDATIONS

5.1 Conclusions

In order to study the effect of chemical liquid deposition, i.e., concentration of TEOS and multicycle silylaltion including with the effect of promoter on characteristic of nano scale Ga/HZSM-5 catalysts for the conversion of n-pentane to aromatics. The results indicated that nano scale HZSM-5 showed the higher aromatic selectivity than parent micro scale HZSM-5 because the presence of mesopore and macropore in nano scale HZSM-5 could improve diffusion of aromatics. Moreover, the addition of Ga with impregnation and ion-exchange method greatly improved the conversion and aromatics selectivity due to the presence of GaO^+ species which acted as Lewis acid site to dehydrogenate cyclic hydrocarbon to aromatics. The impregnated Ga/HZSM-5 showed the lower interaction between gallium and HZSM-5 which easily reduced compared to ion-exchanged Ga/HZSM-5. The effect of TEOS in cyclohexane to silylate Ga/HZSM-5 slightly increased the p-xylene over mixed xylenes but slightly decreased the n-pentane conversion due to the deposition with inert silica layer over external surface of zeolite. The suitable condition with 30% vol TEOS in cyclohexane was used to study in the effect of multicycle silylation. The increase number of cycles in silylation significantly increased the p-xylene selectivity because the multicycle of chemical liquid deposition affected to the formation of uniformity of inert silica layer and increase the amount of inert silica layer. Furthermore, the effect of co-impregnation with promoter to Ga/HZSM-5 showed the different effect to catalytic activity, especially the addition platinum could promote the light alkane formation due to the formation of strong acid sites and the effect of hydrogenolysis. Moreover, co-impregnation with phosphorous increased the aromatics selectivity resulting from the higher medium acid sites fraction including with the pentahedral or dislodged tetrahedral aluminium framework which was new aluminium framework species on zeolite, as be confirmed by ^{27}Al MAS NMR. For these reasons, the highest aromatic selectivity could be obtained from the addition of phosphorous to Ga/HZSM-5.

5.2 Recommendations

The nano scale HZSM-5 showed the good catalytic activity in aromatization of *n*-pentane but exhibited the difficulty in silylation due to the small particles size compared to larger particle sizes. Therefore, choosing the catalyst in industrial field should depend on the product price to reach the highest profit. Moreover, the addition of phosphorus to Ga/HZSM-5 showed the improvement in aromatics selectivity. Thus, the author suggests studying on other precursor, incorporation method and amount of phosphorous to the acidity and acid strength on *n*-pentane aromatization including with the formation of local SAPO interfaces in HZSM-5 zeolite for perspicuous understanding to reach the aims of refineries and petrochemical industry.

REFERENCES

Asaftei, I.V., Bilba, N., Birsa, a.L.M. and Iofceab, G. (2009) Aromatization of industrial feedstock mainly with butanes and butenes over HZSM-5 and Zn/HZSM-5 catalysts. Analytica Chimica Acta 17, 5-34.

Aukett, P.N., Cartlidge, S. and Poplett, I.J.F. (1986) Effect of benzene alkylation on the state of aluminium in zeolite ZSM-5. ZEOLITES 6, 169-174.

Bahatia, S. (1990) Zeolites. Zeolite catalysis principles and application: 239.

Bauer, F., Chen, W.-H., Ernst, H., Huang, S.-J., Freyer, A. and Liu, S.-B. (2004) Selectivity improvement in xylene isomerization. Microporous and Mesoporous Materials 72(1-3), 81-89.

Choudhary, V.R., Mantri, K. and Sivadinarayana, C. (2000) Influence of zeolite factors affecting zeolitic acidity on the propane aromatization activity and selectivity of Ga/H–ZSM-5. Microporous and Mesoporous Materials 37, 1-8.

Danuthai, T., Jongpatiwut, S., Rirksomboon, T., Osuwan, S. and Resasco, D.E. (2006) Aromatization of n-Octane over ZSM-5 Zeolite Catalysts and Its Reaction Pathways. AIChE Annual Meeting.

Engelen, C.W.R., Wolthuizen, J.P. and van Hoof, J.H.C. (1985) REACTIONS OF PROPANE OVER A BIFUNCTIONAL Pt/H-ZSM-5 CATALYST. Applied Catalysis 19, 153-163.

Flanigen, E.M., Broach, R.W. and Wilson, S.T. (2010) Zeolites. Zeolites in Industrial Separation and Catalysis. Kulprathipanja, S., John Wiley & Sons: 1-26.

Gao, Y., Zheng, B., Wu, G., Ma, F. and Liu, C. (2016) Effect of the Si/Al ratio on the performance of hierarchical ZSM-5 zeolites for methanol aromatization. RSC Adv. 6(87), 83581-83588.

Gates, B.C. (1992) Catalytic chemistry, john wiley & sons Ltd.: 270.

Guisnet, M., Gnep, N.S., Aittaleb, D. and Doyemet, Y.J. (1992) Conversion of light alkanes into aromatic hydrocarbons. Applied Catalysis A: General 87, 255-270.

Ihm , S.-K., Yi, K.-H. and Park, Y.-K. (1994) Aromatization of n-pentane over Ni-ZSM-5 catalysts. Studies in Surface Science and Catalysis 84, 1765-1772.

Jacobs, P.A., Flanigen, E.M. and Jansen Herman van Bekkum, J.C. (2001) Studies in Surface Science and Catalysis : Introduction to Zeolite Science and Practice.

Kilic, E. and Yilmaz, S. (2010) HZSM-5 and H-Ferrierite Acidity Modification by Silylation and Their Activities in n-Butene Isomerisation. INTERNATIONAL JOURNAL OF CHEMICAL REACTOR ENGINEERING 8.

Kwak, B.S. and Schachtler, W.H.M. (1994) Effect of Ga/Proton Balance in Ga/HZSM-5 Catalysts on C3 conversion to Aromatics. Catalysis 145, 456-463.

Lai, Y. and Veser, G. (2016) Zn-HZSM-5 catalysts for methane dehydroaromatization. Environmental Progress & Sustainable Energy 35(2), 334-344.

Li, J., Xiang, H., Liu, M., Wang, Q., Zhu, Z. and Hu, Z. (2014) The deactivation mechanism of two typical shape-selective HZSM-5 catalysts for alkylation of toluene with methanol. Catalysis Science & Technology 4(8)

Liang, T., Chen, J., Qin, Z., Li, J., Wang, P., Wang, S., Wang, G., Dong, M., Fan, W. and Wang, J. (2016) Conversion of Methanol to Olefins over H-ZSM-5 Zeolite: Reaction Pathway Is Related to the Framework Aluminum Siting. ACS Catalysis 6(11), 7311-7325.

Liu, J., Zhang, C., Shen, Z., Hua, W., Tang, Y., Shen, W., Yue, Y. and Xu, H. (2009) Methanol to propylene: Effect of phosphorus on a high silica HZSM-5 catalyst. Catalysis Communications 10(11), 1506-1509.

Liu, S., Wu, X., Weng, D., Li, M. and Ran, R. (2015) Roles of Acid Sites on Pt/H-ZSM5 Catalyst in Catalytic Oxidation of Diesel soot. ACS Catalysis 5(2), 909-919.

Long, H., Jin, F., Xiong, G. and Wang, X. (2014) Effect of lanthanum and phosphorus on the aromatization activity of Zn/ZSM-5 in FCC gasoline upgrading. Microporous and Mesoporous Materials 198, 29-34.

Lucas, A.d., Canizares, P., Durhn, A. and Carrero, A. (1997) Dealumination of HZSM-5 zeolites: Effect of steaming on acidity and aromatization activity. Applied Catalysis A: General 154, 221-240.

Meriaudeau, P., Sapaly, G. and Naccache, C. (1991) Dual function mechanism of alkane aromatization over HZSM-5 support Ga, Zn, Pt Catalysts: Respective role of acidity and additive. Studies in Surface Science and Catalysis 60.

Muller, M., Harvey, G. and Prins, R. (2000) Comparison of the dealumination of zeolites beta, mordenite, ZSM-5 and ferrierite by thermal treatment, leaching with oxalic acid and treatment with SiCl4 by 1H, 29Si and 27Al MAS NMR. Microporous and Mesoporous Materials 34, 135-147.

Nakamura, I. and Fujimoto, K. (1996) On the role of gallium for the aromatization of lower paraffins with Ga-promoted ZSM-5 catalysts. Catalysis Today 31(3), 335-344.

Nash, R.J., Dry, M.E. and O' Connor, C.T. (1996) Aromatization of 1-hexene and 1-octene by gallium/H-ZSM-5 catalysts. Applied Catalysis A: General 134, 285-297.

Ni, Y., Sun, A., Wu, X., Hu, J., Li, T. and Li, G. (2011) Aromatization of Methanol over La/Zn/HZSM-5 Catalysts. Chinese Journal of Chemical Engineering 19(3), 439-445.

Nitipan, T., Jongpatiwut, S., Rirksomboon, T., Kitiyanan, B. and Apphakvan, T. (2012) Improved p-Xylene Selectivity of n-Pentane Aromatization over Silylated Ga-exchanged HZSM-5-Catalysts. International Science Index, Chemical and Molecular Engineering 6, 301-304.

Niu, X., Gao, J., Miao, Q., Dong, M., Wang, G., Fan, W., Qin, Z. and Wang, J. (2014) Influence of preparation method on the performance of Zn-containing HZSM-5 catalysts in methanol-to-aromatics. Microporous and Mesoporous Materials 197, 252-261.

Nor, A.S.A. and Didi, D.A. (2003) Characterization and Activity of Cr, Cu and Ga Modified ZSM-5for Direct Conversion of Methane to Liquid Hydrocarbons. Journal of Natural Gas Chemistry 12, 123-134.

Perego, C. (2006) Aromatics. Encyclopaedia of Hydrocarbons: Refining and petrochemicals], ENI. 2.

Pidko, E.A., Hensen, E.J.M. and van Santen, R.A. (2007) Dehydrogenation of Light Alkanes over Isolated Gallyl Ions in Ga/ZSM-5 Zeolites. The Journal of Physical Chemistry C 111(35), 1306813075.

Rane, N., Kersbulck, M., van Santen, R.A. and Hensen, E.J.M. (2008) Cracking of n-heptane over Brønsted acid sites and Lewis acid Ga sites in ZSM-5 zeolite. Microporous and Mesoporous Materials 110(2-3), 279-291.

Rasouli, M., Atashi, H., Mohebbi-Kalhori, D. and Yaghobi, N. (2017) Bifunctional Pt/Fe-ZSM-5 catalyst for xylene isomerization. Journal of the Taiwan Institute of Chemical Engineers 78, 438-446

Rownaghi, A.A., Rezaei, F., Stante, M. and Hedlund, J. (2012) Selective dehydration of methanol to dimethyl ether on ZSM-5 nanocrystals. Appl. Catal. B: Environmental 119–120, 56–61.

SCURRELL, M.S. (1988) Factors affecting the selectivity of the aromatization of light alkanes on modified ZSM-5 catalysts. Applied Catalysis 41, 89-98.

Serra, J., Guillon, E. and Corma, A. (2005) Optimizing the conversion of heavy reformate streams into xylenes with zeolite catalysts by using knowledge base high-throughput experimentation techniques. Journal of Catalysis 232(2), 342-354.

Shao, C.-T., Lang, W.-Z., Yan, X. and Guo, Y.-J. (2017) Catalytic performance of gallium oxide based-catalysts for the propane dehydrogenation reaction: effects of support and loading amount. RSC Adv. 7(8), 4710-4723.

Sirokman, G., Sendoda, Y. and Ono, Y. (1986) Conversion of pentane into aromatics over ZSM-5 zeolites. ZEOLITES 6, 299-303.

Song, W., Justice, R.E., Jones, C.A., V. H. Grassian, V.H. and Larsen, S.C. (2004) Size-Dependent Properties of Nanocrystalline Silicalite Synthesized with Systematically Varied Crystal Size. Langmuir 20, 4696-4702.

Southward, B.W.L., Nash, R.J. and O'Connor, C.T. (1996) In-situ DRIFTS studies of the activation of Ga/H-ZSM-5 catalysts for the aromatization of propane. Applied Catalysis A: General 135, 177-191.

Su, X., Zan, W., Bai, X., Wanga, G. and Wu, W. (2017) Synthesis of microscale and nanoscale ZSM-5zeolites: effect of particle size and acidity of Zn modified ZSM-5 zeolites on aromatization performance. Catalysis Science & Technology 7, 1943-1952.

Tagliabue, M., Carati, A., Flego, C., Millini, R., Perego, C., Pollesel, P., Stocchi, B. and Terzoni, G. (2004) Study on the stability of a Ga/Nd/ZSM-5 aromatisation catalyst. Applied Catalysis A: General 265(1), 23-33.

Teng, H., Wang, J., Ren, X. and Chen, D. (2011) Disproportionation of Toluene by Modified ZSM-5 Zeolite Catalysts with High Shape-selectivity Prepared Using Chemical Liquid Deposition with Tetraethyl Orthosilicate. Chinese Journal of Chemical Engineering 19(2), 292-298.

Todorova, S. and Su, B.-L. (2004) Effects of acidity and combination of Ga and Pt on catalytic behavior of Ga-Pt modified ZSM-5 catalysts in benzene alkylation with pure propane. Catalysis Today 93-95, 417-424.

Todorova, S., Tenchev, K. and Su, B.L. (2005) Benzene alkylation with propane on Ga and Pt modified ZSM-5. Studies in Surface Science and Catalysis 158, 1725-1732.

Tshabalala, T.E. and Scurrell, M.S. (2015) Aromatization of n-hexane over Ga, Mo and Zn modified H-ZSM-5 zeolite catalysts. Catalysis Communications 72, 49-52.

van der Bij, H.E. and Weckhuysen, B.M. (2014) Local silico-aluminophosphate interfaces within phosphated H-ZSM-5 zeolites. Physical Chemistry Chemical Physics 16(21), 9892-9903.

van der Bij, H.E. and Weckhuysen, B.M. (2015) Phosphorus promotion and poisoning in zeolite-based materials: synthesis, characterisation and catalysis. Chemical Society Reviews 44(20), 7406-7428.

Viswanadham, N., Raviraj Kamble, Madhulika Singh, Manoj Kumar and Dhar, G.M. (2009) Catalytic properties of nano-sized ZSM-5 aggregates. Catalysis Today 141, 182-186.

Viswanadham, N., Pradhan, A.R., Ray, N., Vishnoi, S.C., Shanker, U. and Rao, T.S.R.P. (1996) Reaction pathways for the aromatization of paraffins in the presence of H-ZSM-5 and Zn/H-ZSM-5. Applied Catalysis A: General 137, 225-233.

Viswanadham, N. and Saxena, S.K. (2013) Enhanced performance of nano-crystalline ZSM-5 in acetone to gasoline (ATG) reaction. Fuel 105, 490-495.

Weber, R.W., Mo¨ller, K.P., Unger, M. and O'Connor, C.T. (1998) The chemical vapour and liquid deposition of tetraethoxysilane on the external surface of ZSM-5. Microporous and Mesoporous Materials 23, 179-187.

Yue, Y.-H., Tang, Y., Liu, Y. and Gao, Z. (1996) Chemical Liquid Deposition Zeolites with Controlled Pore-Opening Size and Shape-Selective Separation of Isomers. Industrial & Engineering Chemistry Research 35(2), 430-433.

Xiao, H., Zhang, J., Wang, P., Zhang, Z., Zhang, Q., Xie, H., Yang, G., Han, Y. and Tan, Y. (2015) Mechanistic insight to acidity effects of Ga/HZSM-5 on its activity for propane aromatization. RSC Adv. 5(112), 92222-92233.

Zhang, W., Han, X., Liu, X. and Bao, X. (2001) The stability of nanosized HZSM-5 zeolite: a high-resolution solid-state NMR study. Microporous and Mesoporous Materials 50, 13-23.

Zhao, L., Zhu, J., Wang, H.Y., Wei, M., Ma, J. and Bai, Y.Z. (2007) Aromatization of FCC Gasoline Over Modified HZSM-5 Catalyst. Petroleum Science and Technology 25(5), 577-584.

Zheng, S., Heydenrych, H.R., Ro¨ger, H.P., Jentys, A. and Lercher, J.A. (2003) On the Enhanced Selectivity of HZSM-5 Modified by Chemical Liquid Deposition. Catalysis 22, 101-106.

Zheng, S., Jentys, A. and Lercher, J. (2006) Xylene isomerization with surface-modified HZSM-5 zeolite catalysts: An in situ IR study. Journal of Catalysis 241(2), 304-311.

Zhou, G., Lia, J., Yua, Y., Lia, X., Wang, Y., Wang, W. and Komarnenib, S. (2014) Optimizing the distribution of aromatic products from catalytic fastpyrolysis of cellulose by ZSM-5 modification with boron andco-feeding of low-density polyethylene. Applied Catalysis A: General 487, 45-53.

APPENDICES

Appendix A Calculation Activity Testing

Calculation of n-pentane feed flow rate at WHSV = 5 h^{-1}

Amount of HZSM-5 catalyst = 0.20 g

$$\text{WHSV} = \frac{\text{Flow rate } (g \cdot h^{-1})}{\text{Weight of catalyst}}$$

$$5\ h^{-1} = \frac{\text{Flow rate } (g \cdot h^{-1})}{0.20\ g}$$

$$\text{Flow rate} = 1.0\ g \cdot h^{-1}$$

According to n-pentane density is equal to 0.626 g·mL at 20 °C, 1 atm

$$\text{Flow rate} = \frac{1.0\ g \cdot h^{-1}}{0.626\ g \cdot mL}$$

$$= 1.597\ mL \cdot h^{-1}$$

Appendix B Response Factor Calculation

To investigate the response factor of each compound analyzed by a Shimadzu GC-17A, the feed simulation was used. Methane was used as the carrier gas with flowrate at 30 mL/min while the mixed liquid containing pentane, benzene, toluene, m-xylene, o-xylene, and TMB was filled in syringe pump and feed through the reactor with the liquid flowrate at 1.4 mL/min. Then the mix substances were injected to GC and calculated the % actual Area compare with the % theoretical area as shown in Table B1. This method was repeated three times in order to get the average value for the calculation of response factor as shown in Table B2.

Table B1 The calculation of theoretical area

Feed	Density (g/cm^3)	Feed (mL/h)	Feed (g/h)	%Area GC (Theoretical)
Methane	0.000656	1800	1.181	50.85
Pentane	0.626000	0.2	0.125	5.39
Benzene	0.876000	0.2	0.175	7.55
Toluene	0.870000	0.2	0.174	7.49
m-Xylene	0.860000	0.2	0.172	7.41
o-Xylene	0.880000	0.2	0.176	7.58
n-nonane	0.718000	0.2	0.144	6.18
TMB	0.876100	0.2	0.175	7.55

Table B2 Response factor of each compound in the reference standard

Compounds	Residence Time	Response Factor
Methane	1.15	1.06
Pentane[*]	12.53	1.00
Benzene	24.24	1.04
Toluene	30.22	1.03
p-, *m*-Xylene	38.39	1.00
o-Xylene	41.06	0.98

[*]Reference

Appendix C Catalyic Activity Testing

In this part, the conversion and products selectivity in the aromatization of *n*-pentane over parent and modified catalyst were investigated. The reaction conditions were conducted at 500 °C, 1 atm, *n*-pentane flow rate 1.597 mL·h^{-1}, and 5 h^{-1} WHSV. The conversion and products selectivity are shown in Table C1-C5.

Table C1 Conversion and products selectivity over parent micro scale and parent nano scale HZSM-5 in *n*-pentane aromatization at reaction condition: 500 °C, 1 atm, WHSV = 5 h^{-1}, and TOS = 130 min

Products distribution (wt %)	Catalysts	
	Parent Nano HZSM-5	Parent Micro HZSM-5
Conversion (%)	**78.52**	**86.26**
Products Selectivity		
Light paraffins	**63.75**	**70.61**
Methane	3.45	6.73
Ethane	11.07	16.31
Propane	37.79	39.54
Butane	11.44	8.03
Light olefins	**23.31**	**17.87**
Ethylene	8.70	7.27
Propylene	10.19	7.45
Butene	4.41	3.15
Aromatics	**12.94**	**11.52**
Benzene	2.25	3.61
Toluene	6.12	5.53
Ethylbenzene	0.00	0.00
Mixed xylenes	4.57	2.38
***p*-Xylene in xylenes**	**23.10**	**23.80**

Table C2 Conversion and products selectivity over parent nano scale and method of gallium loading to nano scale HZSM-5 in *n*-pentane aromatization at reaction condition: 500 °C, 1 atm, WHSV = 5 h^{-1}, and TOS = 130 min

Products distribution (wt %)	Catalysts		
	Parent Nano HZSM-5	Ga/HZSM-5 (IWI)	Ga/HZSM-5 (IE)
Conversion (%)	**78.52**	**78.48**	**81.77**
Products Selectivity			
Light paraffins	**63.75**	**49.22**	**54.96**
Methane	3.45	7.56	8.63
Ethane	11.07	6.65	6.87
Propane	37.79	22.12	25.86
Butane	11.44	12.89	13.60
Light olefins	**23.31**	**22.84**	**19.22**
Ethylene	8.70	8.77	7.61
Propylene	10.19	9.06	7.46
Butene	4.41	5.02	4.15
Aromatics	**12.94**	**27.94**	**25.82**
Benzene	2.25	7.11	6.90
Toluene	6.12	12.35	12.78
Ethylbenzene	0.00	0.79	0.66
Mixed xylenes	4.57	7.68	5.48
***p*-Xylene in xylenes**	**23.10**	**23.40**	**23.20**

Table C3 Conversion and products selectivity over Ga/HZSM-5 and effect of TEOS loading in silylation to Ga/HZSM-5 in *n*-pentane aromatization at reaction condition: 500 °C, 1 atm, WHSV = 5 h^{-1}, and TOS = 130 min

Products distribution (wt %)	Catalysts			
	Ga/HZSM-5	20CLD/Ga/HZSM-5	30CLD/Ga/HZSM-5	50CLD/Ga/HZSM-5
Conversion (%)	**78.48**	**66.87**	**68.68**	**66.03**
Products Selectivity				
Light paraffins	**49.22**	**51.26**	**49.86**	**50.34**
Methane	7.56	7.69	5.79	8.16
Ethane	6.65	7.09	7.07	6.99
Propane	22.12	22.85	22.85	22.51
Butane	12.89	13.63	14.15	12.68
Light olefins	**22.84**	**26.62**	**23.34**	**26.94**
Ethylene	8.77	10.78	8.33	11.43
Propylene	9.06	10.83	9.20	10.63
Butene	5.02	5.00	5.81	4.88
Aromatics	**27.94**	**22.12**	**26.80**	**22.73**
Benzene	7.11	6.44	6.22	6.56
Toluene	12.35	10.47	12.83	10.39
Ethylbenzene	0.79	0.53	0.79	0.57
Mixed xylenes	7.68	4.68	6.97	5.20
_p_-Xylene in xylenes	**23.40**	**30.25**	**35.00**	**32.89**

Table C4 Conversion and products selectivity over Ga/HZSM-5 and multicycle silylated Ga/HZSM-5 in *n*-pentane aromatization at reaction condition: 500 °C, 1 atm, WHSV = 5 h^{-1}, and TOS = 130 min

Products distribution (wt %)	Catalysts			
	Ga/HZSM-5	30CLD/Ga/ HZSM-5	2C/30CLD/ Ga/HZSM-5	3C/30CLD/ Ga/HZSM-5
Conversion (%)	**78.48**	**68.68**	**50.60**	**22.24**
Products Selectivity				
Light paraffins	**49.22**	**49.86**	**43.84**	**33.85**
Methane	7.56	5.79	5.33	4.90
Ethane	6.65	7.07	6.76	7.75
Propane	22.12	22.85	16.86	12.55
Butane	12.89	14.15	14.89	8.65
Light olefins	**22.84**	**23.34**	**38.63**	**54.13**
Ethylene	8.77	8.33	13.82	19.25
Propylene	9.06	9.20	15.05	25.21
Butene	5.02	5.81	9.75	9.67
Aromatics	**27.94**	**26.80**	**17.53**	**12.02**
Benzene	7.11	6.22	4.29	3.50
Toluene	12.35	12.83	8.70	6.21
Ethylbenzene	0.79	0.79	0.58	0.00
Mixed xylenes	7.68	6.97	3.95	2.31
***p*-Xylene in xylenes**	**23.40**	**35.00**	**69.41**	**100.00**

Table C5 Conversion and products selectivity over Ga/HZSM-5 and promoted Ga/HZSM-5 by co-impregnation method in *n*-pentane aromatization at reaction condition: 500 °C, 1 atm, WHSV = 5 h^{-1}, and TOS = 130 min

Products distribution (wt %)	Catalysts				
	Ga/HZSM-5	0.2PtGa/ HZSM-5	0.2ZnGa/ HZSM-5	0.2LaGa/ HZSM-5	0.2PGa/ HZSM-5
Conversion (%)	**78.48**	**99.04**	**74.88**	**78.04**	**73.92**
Products Selectivity					
Light paraffins	**49.22**	**93.09**	**54.58**	**50.83**	**39.56**
Methane	7.56	7.40	8.19	7.62	4.77
Ethane	6.65	40.50	9.59	7.43	7.14
Propane	22.12	43.31	23.83	23.95	19.55
Butane	12.89	1.89	12.97	11.82	8.09
Light olefins	**22.84**	**2.00**	**23.61**	**20.38**	**18.15**
Ethylene	8.77	0.00	9.14	7.94	6.99
Propylene	9.06	2.00	9.20	7.87	7.19
Butene	5.02	0.00	5.26	4.57	3.96
Aromatics	**27.94**	**4.91**	**21.81**	**28.80**	**42.29**
Benzene	7.11	2.25	5.85	7.05	8.94
Toluene	12.35	2.01	10.32	13.39	19.69
Ethylbenzene	0.79	0.00	0.54	0.76	1.10
Mixed xylenes	7.68	0.65	5.10	7.60	12.57

CURRICULUM VITAE

Name: Mr. Sukkatad Sintapanin

Date of Birth: December 10, 1993

Nationality: Thai

University Education:

2012–2015   Bachelor Degree of Science Chemical Technology, Faculty of Science, Chulalongkorn University, Bangkok, Thailand.

Work Experience:

2015   Position: Trainee

             Company name: Mitr Phol Biofuel Company Limited.